Projections of Auditory Cortex to the Medial Geniculate Body of the Cat

JEFFERY A. WINER,* **JAMES J. DIEHL,** AND **DAVID T. LARUE**
Division of Neurobiology, Department of Molecular and Cell Biology, University of
California at Berkeley, Berkeley, California 94720-3200

ABSTRACT

The corticofugal projection from 12 auditory cortical fields onto the medial geniculate body was investigated in adult cats by using wheat germ agglutinin conjugated to horseradish peroxidase or biotinylated dextran amines. The chief goals were to determine the degree of divergence from single cortical fields, the pattern of convergence from several fields onto a single nucleus, the extent of reciprocal relations between corticothalamic and thalamocortical connections, and to contrast and compare the patterns of auditory corticogeniculate projections with corticofugal input to the inferior colliculus. The main findings were that (1) single areas showed a wide range of divergence, projecting to as few as 5, and to as many as 15, thalamic nuclei; (2) most nuclei received projections from approximately five cortical areas, whereas others were the target of as few as three areas; (3) there was global corticothalamic-thalamocortical reciprocity in every experiment, and there were also significant instances of nonreciprocal projections, with the corticothalamic input often more extensive; (4) the corticothalamic projection was far stronger and more divergent than the corticocollicular projection from the same areas, suggesting that the thalamus and the inferior colliculus receive differential degrees of corticofugal control; (5) cochleotopically organized areas had fewer corticothalamic projections than fields in which tonotopy was not a primary feature; and (6) all corticothalamic projections were topographic, focal, and clustered, indicating that areas with limited cochleotopic organization still have some internal spatial arrangement. The areas with the most divergent corticothalamic projections were polysensory regions in the posterior ectosylvian gyrus. The projection patterns were indistinguishable for the two tracers. These findings suggest that every auditory thalamic nucleus is under some degree of descending control. Many of the projections preserve the relations between cochleotopically organized thalamic and auditory areas, and suggest topographic relations between nontonotopic areas and nuclei. The collective size of the corticothalamic system suggests that both lemniscal and extralemniscal auditory thalamic nuclei receive significant corticofugal input. J. Comp. Neurol. 430:27–55, 2001.   © 2001 Wiley-Liss, Inc.

Indexing terms: corticofugal; corticogeniculate; corticothalamic system

The classic view of sensory processing in the mammalian brain postulates a serial sequence of synaptic input that begins with the peripheral receptor, whose associated ganglion cells project to one or more subcortical stations, in which a map of the sensory epithelium is established. The output of this initial central neural representation subsequently passes through subcortical nuclei in the brain stem and thalamus before it terminates in one or more cortical areas, where a topographic functional representation of the receptor mosaic is expanded and elaborated for analytical and computational purposes (Jones, 1985). This paradigm has been enlarged by the idea that corticofugal projections play a complementary, and perhaps even an executive, role in the control of subcortical

excitability (Przybyszewski, 1998). The evidence available suggests that the corticothalamic projections are among the larger connectional systems in the brain (Winer and Larue, 1987). Although the significance of corticothalamic projections has been recognized, the lack of detailed phys-

iological evidence has, until rather recently, relegated them to a position in which their feedback role was emphasized (Frigyesi et al., 1972). It came as something of a surprise, then, to find that corticothalamic projections have functional roles in diverse thalamic operations, and that their influences in the visual system, for example, range from enhanced information processing (McClurkin et al., 1994), to precise regulation of the temporal discharge structure of thalamocortical neurons (Funke et al., 1996; Wörgötter et al., 1998), and the modulation of orientation-discontinuity-sensitive lateral geniculate neurons (Cudeiro and Sillito, 1996), to name just a few. The range of physiologic operations under implicit cortical control, thus, is much larger than a term such as feedback might seem to suggest. The purpose of the present study is to reinvestigate the auditory corticothalamic (CT) projec-

tions by using the most sensitive tract-tracing methods now available, and to include the many auditory areas now recognized in the cat neocortex (Reale and Imig, 1980; Winer, 1992).

Construing the thalamus as a relay nucleus whose principal task is to preserve peripheral input and convey it to the cortex vastly oversimplifies its many roles in transforming and integrating ascending information (Winer et al., 1996; Yan and Suga, 1996a,b; Fitzpatrick et al., 1997). The proposition that the CT system provides reafference to the thalamus begs the very question that it presumes to answer because this prospective feedback probably exceeds in size the corresponding thalamocortical projection itself. The present study is part of a larger investigation that addresses the structure, connections, and neurochemical organization of layers V and VI to provide a

---

Abbreviations

AAF	anterior auditory field		Ov	ovoid part of the ventral division of the medial geniculate body
aes	anterior ectosylvian sulcus		P	posterior auditory cortex
AI	primary auditory cortex		PC	posterior commissure
AII	second auditory cortical area		pes	posterior ectosylvian sulcus
als	anterior lateral sulcus		PL	posterior limitans nucleus
ans	ansate sulcus		pls	posterior lateral sulcus
AP	anterior paraventricular nucleus		PN	paracentral nucleus
APt	anterior pretectal nucleus		Pol	posterior area of the thalamus, lateral nucleus
as	anterior suprasylvian sulcus		Pom	posterior area of the thalamus, medial nucleus
BIC	brachium of the inferior colliculus		Pul	pulvinar
BSC	brachium of the superior colliculus		Pf	parafascicular nucleus
CC	caudal cortex of the inferior colliculus		ps	pseudosylvian sulcus
CG	central gray		pss	posterior sylvian sulcus
CIC	commissure of the inferior colliculus		Pt	pretectum
CL	central lateral nucleus		Py	pyramidal tract and corticobulbar fibers
CM	centre médian nucleus		Rh	rhomboid nucleus
CMN	central medial nucleus		RN	red nucleus
CN	central nucleus		RP	rostral pole nucleus of the inferior colliculus
cos	coronal sulcus		RR	retrorubral field
cs	cruciate sulcus		rs	rhinal sulcus
CP	cerebral peduncle		RtN	thalamic reticular nucleus
Cu	cuneiform nucleus		Sa	nucleus sagulum
D	dorsal nucleus of the medial geniculate body		SC	superior colliculus
DCa	dorsal caudal division of the medial geniculate body		SF	suprasylvian fringe auditory cortex
DCI-IV	layers of the dorsal cortex of the inferior colliculus		Sgl	suprageniculate nucleus, lateral part
DD	deep dorsal nucleus of the medial geniculate body		Sgm	suprageniculate nucleus, medial part
DS	dorsal superficial nucleus of the medial geniculate body		SN	substantia nigra
EP	posterior ectosylvian gyrus		SNc	substantia nigra, *pars compacta*
EPD	posterior ectosylvian gyrus, dorsal part		SNr	substantia nigra, *pars reticulata*
EPI	posterior ectosylvian gyrus, intermediate part		Spf	subparafascicular nucleus
EPP	posterior ectosylvian gyrus, posterior part		Spfm	subparafascicular nucleus, medial part
EPV	posterior ectosylvian gyrus, ventral part		SpN	suprapeduncular nucleus
Fx	fornix		St	subthalamic nucleus
Ha	habenula		Spf	subparafascicular nucleus
HDA	hypothalamus, dorsal area		Te	temporal cortex
HPA	hypothalamus, posterior area		Tr	trochlear nucleus
HiT	habenulointerpeduncular tract		V	lateral part of the ventral division of the medial geniculate body
HLA	hypothalamus, lateral area		Ve	ventral auditory cortex
IcT	intercollicular tegmentum		Vb	ventrobasal complex
ICP	inferior cerebellar peduncle		Vl	ventrolateral nucleus of the medial geniculate body
Ins	insular cortex		VP	ventral posterior auditory cortex
LD	lateral dorsal nucleus		Vpl	ventroposterolateral nucleus
LGB	lateral geniculate body		Vpm	ventroposteromedial nucleus
LMN	lateral mesencephalic nucleus		ZI	zona incerta
LN	lateral nucleus of the inferior colliculus		I–IV	layers of the dorsal cortex of the inferior colliculus
LP	lateral posterior nucleus			Planes of section:
M	medial division of the medial geniculate body		C	caudal
MB	mammilary body		D	dorsal
MCP	middle cerebellar peduncle		L	lateral
MD	medial dorsal nucleus		M	medial
MRF	mesencephalic reticular formation		R	rostral
mss	middle suprasylvian sulcus			Nonauditory cortical areas:
MZ	marginal zone of the medial geniculate body			3,4,5,6,7,8,17,18,19,20a,21a,SI,SII
NBIC	nucleus of the brachium of the inferior colliculus			
OT	optic tract			

context for a more balanced picture of the corticofugal auditory system (Winer et al., 1998, 1999; Prieto and Winer, 1999).

Refinements in knowledge of the principal circuitry in the thalamocortical (TC) system has not been matched by a corresponding level of detail about the CT pathway, whose experimental analysis has had a much shorter history (Frigyesi et al., 1972; Jones, 1985). It was possible to question, only a few years ago, with the methods then available, whether primates had an auditory CT projection (Krieg, 1963). Subsequent work has shown that it is present robustly (Pandya et al., 1994) and reciprocates TC projections (Mesulam and Pandya, 1973; Hashikawa et al., 1995). Nevertheless, the precise role of the CT system remains somewhat enigmatic, and the necessity for so massive a projection is unknown.

Parallels in CT organization between the auditory and visual system may reveal the basic principles of CT organization. For example, the feline medial geniculate body has three divisions and ≈12 nuclei (Winer, 1992), some without a precise analogue in the visual thalamus (Stone, 1983). Therefore, it is pertinent to ask how many patterns of CT input exist within and between modalities. A second goal is to reexamine the auditory CT system with regard to the several (more than 10) regions now recognized as auditory cortex (Reale and Imig, 1980). For example, does every area with a precise cochleotopic organization have the same CT targets? A third goal is to clarify the arrangement of divergent or convergent projections in the CT system. A projection from one area to many thalamic nuclei suggests that cortical feedback is essential for some global aspect of sound processing. A fourth task is to explore the rules governing TC-CT reciprocity, with special reference to the many nonprimary cortical areas in which a cochleotopic organization is attenuated or absent (Clarey et al., 1992). Differences in projections between tonotopic and nontonotopic areas could suggest areally specific patterns of corticofugal control. Finally, these results will serve as a framework to compare the auditory corticogeniculate projection with the parallel input to the inferior colliculus (Winer et al., 1998) and other midbrain targets (Beneyto et al., 1998); such data will be useful in deriving a more complete profile of the corticofugal system.

A further goal is to integrate the many features of auditory corticofugal organization into a larger picture of thalamic function. For example, any complete theory would have to consider which types of neuron in layers V and VI project in the corticofugal system (Kelly and Wong, 1981), and the nature of any sublaminar differences in the origins of these neurons (Fitzpatrick et al., 1994). Finally, it remains to delineate which cortical areas project to particular thalamic nuclei. Moreover, the shared and salient features in the structure of CT axon terminals from primary and nonprimary auditory cortex depend on such studies. These data suggest that differences in size, shape, density, and postsynaptic targets may have different functional consequences. It is unknown which features are conserved between cortical areas and thalamic targets.

MATERIALS AND METHODS

Adult cats of either sex and free of middle ear disease were used. Males with white coats and blue eyes and Siamese cats were excluded. Animal care and husbandry was administered under veterinary supervision, and the experimental and surgical protocols were approved by an institutional animal care and use committee. Standard guidelines for basic care were followed (Society for Neuroscience, 1991).

Wheat germ agglutinin conjugated to horseradish peroxidase (WGA-HRP) was injected in one series of experiments and biotinylated dextran amines (BDA) in another set to confirm the WGA-HRP results and to label corticothalamic axons by diffusion so that their morphology could be visualized; the latter results will be reported separately. Forty-one hemispheres were available for study (Winer et al., 1998).

Surgery

All procedures were carried out by using sterile technique on cats older than 8 months. The subjects were sedated with acepromazine (0.2 mg/kg, s.c.) then induced and maintained under isoflurane (1–3% and O_2) after intubation. The level of anesthesia was adjusted to suppress corneal and pedal reflexes, and its depth was assessed by continuous monitoring of respiration, arterial O_2, core temperature, and electrocardiogram. Hydration was maintained with lactated Ringer's solution (≈10 ml/kg/hour, i.v.), and body temperature was stabilized with a warm water pad (34–39°C). The corneas were coated with ophthalmic ointment to prevent desiccation.

A craniotomy exposed gyral and sulcal landmarks (Fig. 1A) that were used to target the deposits, because they approximate the location of particular architectonic fields (Rose and Woolsey, 1949; Winer, 1992) as defined by tract-tracing and physiologic studies (Reale and Imig, 1980; Bowman and Olson, 1988a,b). Tracer was injected unilaterally because some corticofugal projections are bilateral (Andersen et al., 1980b). The WGA-HRP (5%) was dissolved in sterile saline and the BDA (10–20%) in distilled water. Deposits (Fig. 1B) were made with a glass pipet (25- to 35-μm tip diameter) at 300- to 400-μm intervals through the cortical depth to saturate all layers and label the corticothalamic (Prieto and Winer, 1999) and the thalamocortical (Sousa-Pinto, 1973; Huang and Winer, 2000) projections in their entirety (Winer, 1992, p. 304). A nanoliter hydraulic pump (World Precision Instruments, Sarasota, FL) ejected tracer in pulses (4.6 or 9.2 nL every 30–120 seconds/10–32 minutes) to achieve final volumes of 0.08–2.07 μl. In two experiments, iontophoresis was used to deliver BDA dissolved in saline with a 5 μA alternating positive current for 15–20 minutes on a 7-second duty cycle. For WGA-HRP, survivals were 1–4 days, with all periods equally effective. For BDA, 7- to 28-day survivals were used, with 7–15 days proving optimal. Postoperatively, the animal received a synthetic narcotic analgesic (buprenorphine; 0.00875–0.0125 mg/kg; s.c.) for 1–2 days.

Histology

Animals were anesthetized for perfusion with sodium pentobarbital (26 mg/kg, i.v.) and perfused through the heart. For WGA-HRP experiments, the washout (0.12 M phosphate buffer [PB], the vehicle for all solutions, with 0.001% lidocaine hydrochloride, 250–400 ml, pH 7.4, 24°C) was followed by a weak first fixative (0.5% paraformaldehyde/0.5% glutaraldehyde/PB, 1,000 ml, 4–10°C), then a second fixative (1% paraformaldehyde/1.5% glutaraldehyde, 2,250 ml, 4–10°C). The procedure
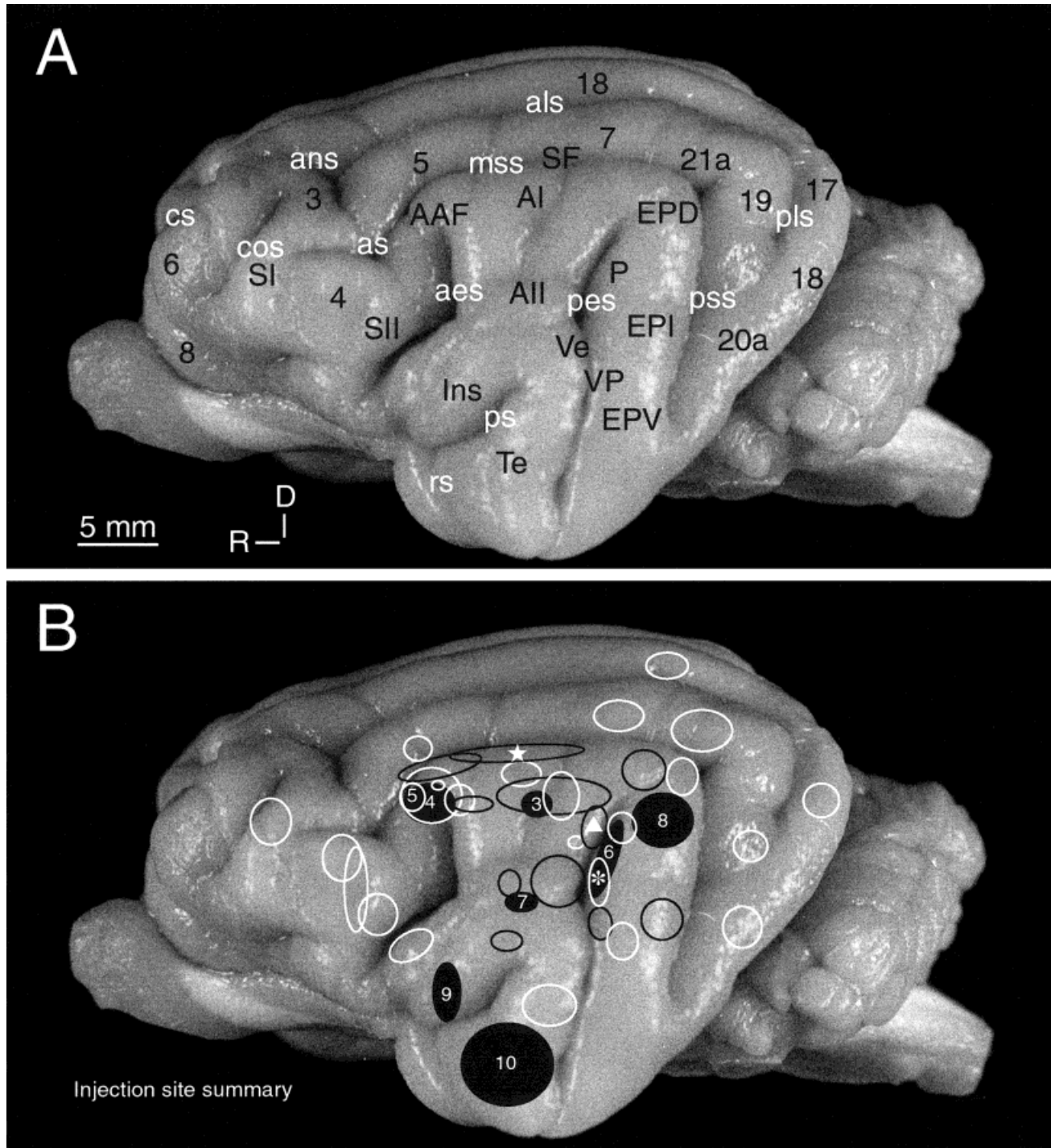
Fig. 1. Cortical subdivisions and composite view of injection sites. **A:** Representative hemisphere on which the major sulci (white letters) and the principal architectonic fields (black letters) have been denoted. The deposits (panel B) were targeted by using the sulcal pattern as a guide (Kawamura, 1971) and with reference to physiological studies (Rose and Woolsey, 1949; Reale and Imig, 1980). The major auditory cortical areas were identified in Nissl preparations, whereas the visual fields were defined by reference to other studies (Tusa et al., 1981). Protocol for A, B: 35-mm macrophotographic negatives were scanned (Nikon LS-1000), imported into a graphics program (Adobe Photoshop 4.0), composed and labeled (Adobe Illustrator 7.0), then printed (Fargo Pictura™ 310 dye sublimation process). Images were edited to eliminate blocking cuts and to reduce background. SI, primary somatic sensory cortex; SII, second somatic sensory cortex. Numbers, areal subdivisions of sensorimotor neocrotex. **B:** Cortical injection sites (oval profiles). Numbers refer to figures from illustrated experiments. Black filled profiles represent deposit sites in cases using wheat germ agglutinin conjugated to horseradish peroxidase (WGA-HRP), from which most of the data shown here were taken. Open black profiles are WGA-HRP cases that are not illustrated further. Open white profiles denote injections with biotinylated dextran amines (BDA), of which one (#5) is presented. The corresponding BDA deposits in other experiments were smaller but had much the same distribution of terminal labeling (compare Figs. 4, 5). Auditory-responsive cortex had an area ≈500 mm² in adult animals when sulcal cortex was included (Winer, 1992). The criteria for selection for analysis were that the deposit should be remote from architectonic borders, that it did not invade the white matter significantly, and that the cat had a relatively normal sulcal and gyral pattern. For abbreviations in this and all subsequent figures, see list.

was similar for BDA except that a different fixative (4% paraformaldehyde, pH 7.4) was used. A cryoprotectant solution (10% sucrose/PB, 500 ml, 4–10°C) was perfused 1 hour later, after which the head was removed, mounted in a stereotaxic frame, and blocked in the frontal plane; a 24-mm-long transverse slab was prepared that included a region from the inferior colliculus to the anterior striatum. The brain was photographed in the cardinal planes and stored in cryoprotectant (30% sucrose/PB, 1–3 days).

For WGA-HRP histochemistry, 60-μm-thick frozen sections were cut on a sliding microtome and collected in a series of six in chilled 0.1 M PB. Three sections were processed with tetramethylbenzidine (TMB), and one was counterstained with neutral red (Mesulam, 1978). The deposits were located in the TMB material and nearby sections were reacted in nickel/cobalt-intensified diamino-benzidine (DAB) (Adams, 1981) to provide a more accurate estimate of the effective limits of the injections. A set of unreacted sections was mounted, and these and the DAB-processed material were stained for Nissl substance or post-fixed in 10% formalin (5–10 days) before Nissl staining.

For BDA experiments, 50-μm-thick frozen sections were cut and collected as noted above. Some sections were permeabilized briefly (0.3–0.4% Triton X-100) then incubated in avidin biotin complex (ABC Elite reagent, Vector Laboratories, Burlingame, CA). After this, the biotin-peroxidase signal was visualized by using heavy metal-intensification (Adams, 1981). A 1:3 Nissl series was prepared for cytoarchitectonic examination.

Data analysis

From each experiment, approximately 12 sections were chosen that represented the caudorostral distribution of labeling throughout the thalamus. Low-power drawings were prepared from which the sections chosen for illustration were selected. The thalamic subdivisions (Fig. 2) were drawn separately from the Nissl preparations, and the two results were compared and any discrepancies reconciled. In these, the anterogradely labeled axon terminals (Figs. 3–10: fine dots) and the retrogradely labeled neurons (Figs. 3–10: circles) were charted at 125× through a drawing tube by using darkfield illumination. Cortical regions were defined in the Nissl preparations (for details, see Winer et al., 1998).

RESULTS

Auditory thalamic architectonic subdivisions

To provide a context for the experimental results, the main target nuclei will be described briefly in Nissl and myeloarchitectonic preparations. The scheme used incorporates cytoarchitectonic observations (Berman and Jones, 1982) and the results from studies of thalamocortical (Niimi and Matsuoka, 1979) and corticothalamic (Pontes et al., 1975) projections. Golgi material provided information about neuronal architecture and the form and distribution of the various axonal populations that define the myeloarchitectonic profile (Morest, 1964, 1965; Winer and Morest, 1983a,b, 1984).

Ventral division. This large nucleus extends from the caudal one-fifth (Fig. 2C: V) to just behind the rostral pole (Fig. 2E) of the auditory thalamus. It contains bushy tufted neurons (Morest, 1964) that project to the primary auditory cortex (Winer, 1984) and a smaller intrinsic neuron (Morest, 1971) that is gamma-aminobutyric acid-positive (GABAergic; Huang et al., 1999). The principal cells form long fibrodendritic laminae that run from dorsolateral-to-ventromedial, and across which is imposed a systematic arrangement of characteristic frequency oriented along the lateromedial axis (Aitkin and Webster, 1972). This organization is clearest in the most lateral, low-frequency subdivision, the *pars lateralis* (Fig. 2E: V), whereas neurons in the more medial *pars ovoidea* (Fig. 2C: Ov) form much shorter and more irregular rows as a result of the compression of the laminae that transform the local fiber architecture. The brachium of the inferior colliculus (Fig. 2: BIC) moves progressively more laterally along the posterior-to-anterior axis, effectively dividing the ventral division into lateral and medial territories.

Dorsal division. This is an architectonically diverse region containing at least six nuclei, and it extends almost the entire length of the auditory thalamus. The neurons are packed less densely than those of the ventral division. The fiber architecture is dominated by extremely fine axons (Fig. 2D). The principal parts are the dorsal nuclei proper, including the dorsal superficial (DS), dorsal (D), and deep dorsal (DD); these project to the second auditory cortex (Fig. 1A: AII) and to insular (Ins) and temporal (Te) fields (Winer et al., 1977). There are two types of principal neurons, radiate and tufted (Winer and Morest, 1983b, 1984), and there is a small (Rouiller et al., 1990) and a large (Huang et al., 1999; Winer et al., 1999) cell type that are GABAergic. There is little evidence for a tonotopic representation, and the neurons are tuned broadly (Aitkin and Dunlop, 1968; Aitkin and Prain, 1974). The supra-geniculate nucleus has lateral (Fig. 2C: Sgl) and medial (Fig. 2E: Sgm) subdivisions. These neurons are polysensory (Benedek et al., 1996) and project to the insulotemporal cortex (Clascá et al., 1997), the caudate nucleus (Hu and Jayarman, 1986), and the frontal lobe (Casseday et al., 1989). The ventrolateral nucleus (Fig. 2E: Vl) is present from the caudal tip to the rostral three-fourths of the auditory thalamus and has widespread connections with many nonprimary cortical areas (Winer et al., 1977, 1999). The status of the caudal dorsal nucleus (Fig. 2A: DCa) is uncertain: its neurons resemble those elsewhere in the dorsal division (Winer and Morest, 1983b, 1984), but differ somewhat in their cortical connections (present results).

Medial division. These neurons are heterogeneous in size and shape (Winer and Morest, 1983a) and they project widely to both auditory (Winer et al., 1977) and nonauditory (Jones and Powell, 1973) cortex. This division is present through the caudorostral extent of the auditory thalamus, except at the most rostral pole. Large, heavily myelinated axons predominate (Fig. 2F; Saint Marie et al., 1997). Although the tuning curves of single neurons are broad (Aitkin, 1973), there is a systematic, caudorostral frequency progression from low to high (Rouiller et al., 1989) that is less orderly than that in the ventral division. Like the other parts of the medial geniculate body, it contains many local circuit neurons (Winer, 1992), and these correspond closely to the profiles of GABAergic cells (Rouiller et al., 1990; Huang, 1999; Huang et al., 1999).

Corticothalamic projections

Among the features shared by all experiments were that (1) injections confined to one cortical architectonic field
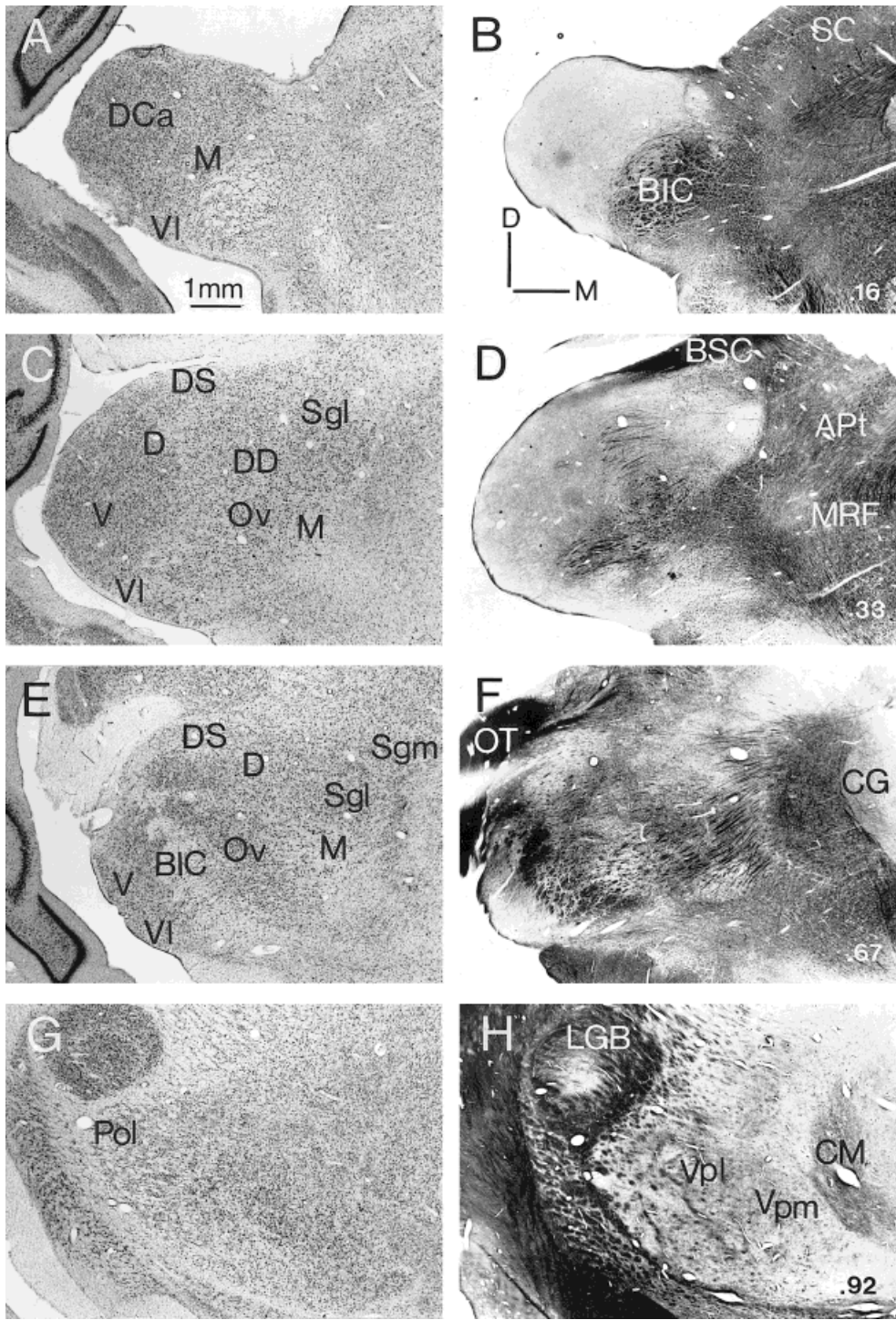
Figure 2

always labeled several thalamic nuclei; (2) even relatively small cortical deposits labeled much of the caudorostral extent of single nuclei; (3) there were significant zones of corticothalamic-thalamocortical reciprocity, and somewhat smaller regions of nonreciprocity; (4) thalamic nuclei without known internal functional topography nevertheless have a high degree of connectional order. Each experiment was repeated at least once by using a different tracer; a particular case was accepted for analysis only if the deposits did not cross architectonic borders and if the intended replication(s) were confirmatory. The term *mixed* refers to overlapping corticothalamic and thalamocortical projections in a nucleus.

Area AI. Four experiments (three with WGA-HRP, one with BDA) were available. Because the results in each were similar, only one case was chosen for illustrative purposes (Fig. 3). The WGA-HRP injection was centered in the primary auditory cortex, area AI (Fig. 3A), in the middle ectosylvian gyrus, remote from the boundary with the dorsal part of the posterior ectosylvian gyrus (Fig. 1A: EPD) and far from area AII (Fig. 3A: AII). The 2-mm-long deposits diffused slightly into the white matter (Fig. 3B: stipple).

The most prominent auditory thalamic labeling was in the ventral division of the medial geniculate body (Fig. 3E: V), a projection that extended through most of the caudorostral axis (Fig. 3C–G: V). The band of mixed labeling included axon terminals and retrogradely labeled neuronal perikarya, and instances of either type alone. The projection began as a dense focus caudally (Fig. 3C) then expanded until it filled the central half of the ventral division (Fig. 3E: V), sparing most of the more medial *pars ovoidea* (Fig. 3E,F: Ov). There was moderate labeling, mainly of fibers, in the dorsal nucleus (Fig. 3F: D), and sparse input to the dorsal superficial nucleus (Fig. 3G: DS). Even at this comparatively rostral level (0.72% from the caudal tip of the auditory thalamus), the mediolateral position of the transport was consistent as the thalamic contour changed gradually in shape. In the most rostral section (Fig. 3H, 0.81%; Fig. 12A), the projection was still lighter, whereas its mediolateral position was preserved. The virtual absence of fibers of passage here, and the

massive concentration of terminal input more caudally, suggest that the granular WGA-HRP material represents mainly axonal boutons and that most fibers of passage were detected and excluded consistently. This observation confirms the results of autoradiographic studies of the rat CT projection (Winer and Larue, 1987). Another feature was the labeling at the junction of the *pars ovoidea* and the medial division (Fig. 3C,D: Ov,M), which was interpreted as a light input to the latter, because the locus of injection and of retrograde labeling make it unlikely that cortical regions besides AI were involved.

Area AAF. The anterior auditory field is rostral to AI and has a cochleotopic organization, which is inverted relative to that in AI, with the highest frequencies caudally (Knight, 1977). With few exceptions, the distribution of CT labeling was indistinguishable from that arising from AI (Fig. 14: AI,AAF). Five experiments were available with deposits confined to AAF. Two cases were chosen for illustration, one of which used WGA-HRP (Fig. 4), the other BDA (Fig. 5); this approach provided an independent check on the consistency of the results by comparing the two tracers. The AAF deposit (Fig. 4A), although apparently larger than the AI injection (Fig. 3A), was considered as confined to AAF on several grounds. (1) The cytoarchitecture matched that of AAF in other studies (Winer, 1992, Fig. 6.8E). (2) The most extensive labeling was in the more lateral, low-frequency parts of the ventral division (Aitkin and Webster, 1972), which is ≈7 mm or more from the matching AI representation (Rose and Woolsey, 1949). (3) It is unlikely that any substantial number of low-frequency thalamocortical fibers ascending to AI would first turn rostrally, and then project caudally. (4) There was no anterograde labeling in the superior colliculus (Fig. 15B: SC), which might have been expected (Meredith and Clemo, 1989) had the deposit encroached upon the anterior ectosylvian gyrus (Fig. 1A: aes). (5) The auditory thalamic labeling was concentrated in the central part of the ventral division, in accord with the architectonic interpretation that the central two-thirds (middle frequency parts) of AAF were involved.

The caudal foci of projection (Fig. 4C) were patchy and discontinuous. A few labeled somata without correspond-

Fig. 2. Medial geniculate body cyto- and myeloarchitecture. A,C,E,G: Nissl preparations. Planapochromat, N.A. 0.04, ×16. B,D,F,H: Osmicated, epoxy embedded whole-mounts. All sections were 50 µm thick. Decimals at lower right (B,D,F,H) refer to the percentage distance from tip of the caudal pole of the medial geniculate body in this and subsequent figures. **A,B:** At 16% from the caudal tip, only nuclei of the dorsal and medial divisions were present. The caudal dorsal nucleus (DCa) extends to, and forms, the posterior face of the auditory thalamus. Its loosely packed multipolar neurons were embedded in a plexus of fine, myelinated fibers, many arising from the brachium of the inferior colliculus (BIC) The ventrolateral nucleus (Vl) was a compact mass that extended rostrally to ≈70%, with an unusually pale myeloarchitecture. Medial division (M) neurons were dispersed among fascicles of brachial axons. The magnocellular neurons were prominent here and less numerous more rostrally. Posterior intralaminar nuclei were interposed as thin strips between the brachium and the underlying cerebral peduncle, and their long axis was oriented mediolaterally. **C,D:** The dorsal division nuclei became prominent and the ventral division was at near-maximum size. The superficial dorsal nucleus (DS) was a shell oriented mediolaterally on the perimeter of the free surface of the auditory thalamus; many of its neurons had their dendrites polarized along this orientation. Large

bundles of myelinated axons traversed the dorsal division. Its medial border was the suprageniculate nucleus (lateral part; Sgl), whose principal cells were second in size only to those of the medial division, and which had a radiating dendritic configuration. The inferior boundary was the dorsal nucleus (D), with neurons packed more densely; these cells had a radiate or a tufted dendritic architecture. Deep dorsal nucleus (DD) cells stained more darkly than other dorsal division neurons, and they formed an oval cluster of densely packed neurons between the dorsal nucleus (dorsally), the suprageniculate nucleus (medially), and the *pars ovoidea* (ventrally). Ventral division neurons formed vertical rows in the *pars lateralis* (V) and had a less ordered arrangement in the more medial *pars ovoidea* (Ov), whose laminar organization was disrupted by brachial fibers (BIC). **E,F:** A second subdivision of the suprageniculate nucleus, the medial part (Sgm) extended from the lateral part (Sgl) to the midline. The inferior brachium here contained thalamofugal as well as corticothalamic axons. **G,H:** The rostral pole (>80%) has not been examined in Golgi preparations; it was bordered by the anterior pole of the lateral geniculate body (dorsally), the thalamic reticular nucleus (laterally), the ventrobasal complex (medially), and parts of the optic tract and subthalamic territories (rostrally). For abbreviations, see list. Scale bar in A and orientation in B applies to all panels.
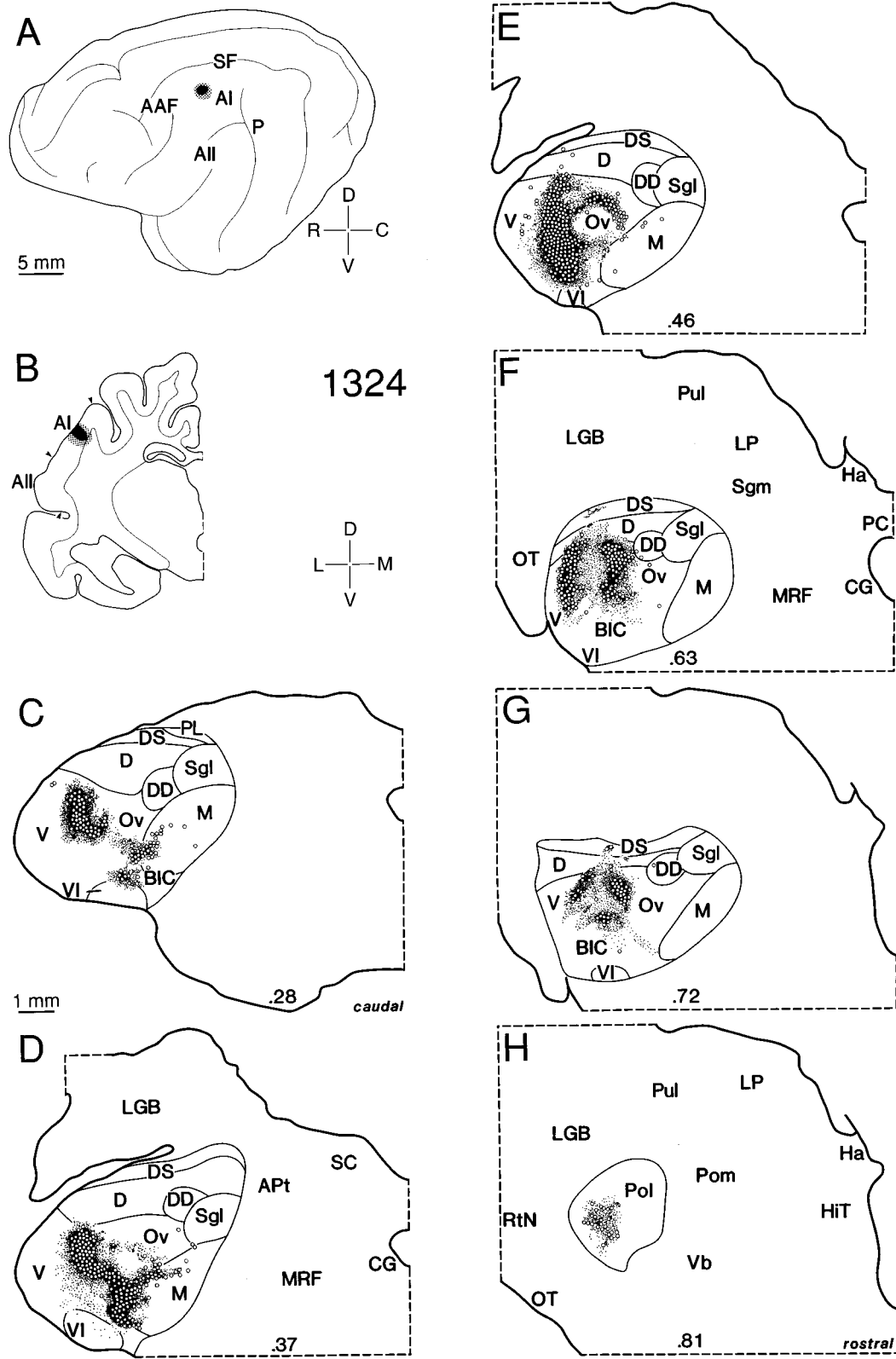
Fig. 3. Corticothalamic and thalamocortical projections of area AI. **A:** Reconstructed hemisphere from a lateral perspective. Black area, effective injection site; stippled area, zone of tracer diffusion. **B:** Coronal section through the center of the injection sites. Arrowheads, cytoarchitectonic borders. C–G: Terminal anterograde labeling (fine stippling) and cells of origin (small open circles) from representative sections. Projections are ipsilateral only. The main results in this experiment were that the projection was topographical and the labeling was concentrated in the center of the ventral division, that the terminals and the cells of origin largely overlapped, and that the rostral pole (Pol) contained significant terminal labeling. **C:** The projection consisted of a focal mass of mixed labeling that was largely continuous through the auditory thalamus. **D:** Scattered cells of origin occurred in the medial division (M: panels C–E). **E:** The injection site was ≈2 mm tall and the band of retrograde labeling in the ventral division was >3 mm, suggesting that massive thalamocortical convergence and significant corticothalamic divergence were present. The convergence of descending input and the divergent projections of the cells of origin are scaled relative to each other. **F:** At its maximum size, the brachium of the inferior colliculus (BIC: see Fig. 2F, 0.67%) divided the medial division. **G:** Small foci, chiefly of anterograde labeling, extended into the anterior nuclei of the dorsal division and throughout the ventralmost *pars ovoidea*. **H:** Even light projections were highly reciprocal. Protocol for Figures 3–11: Planachromat, N.A. 0.13, ×15. Subdivisions drawn from adjacent, Nissl-stained preparations.
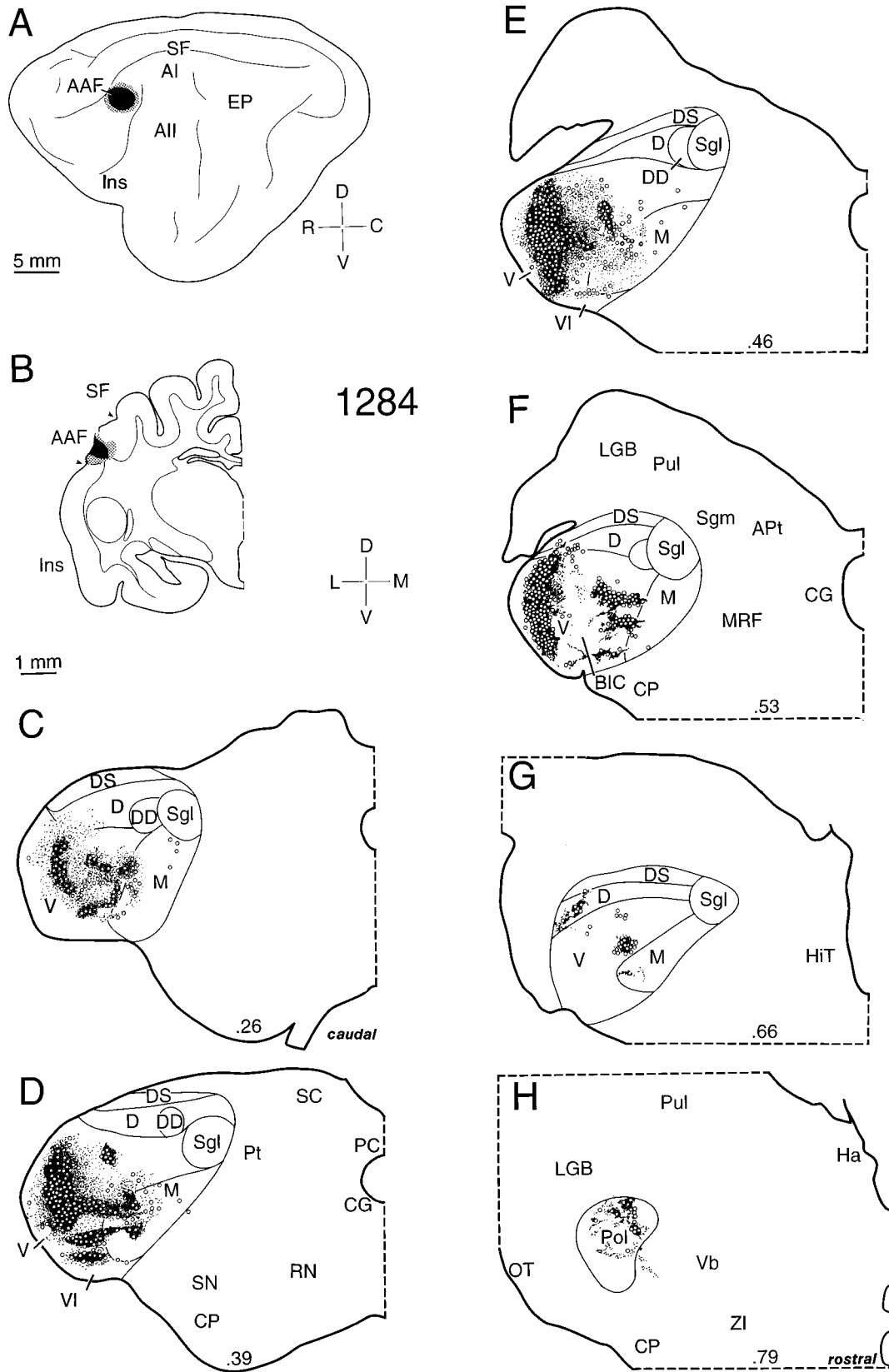
Fig. 4. Connections of area AAF revealed by wheat germ aggluti-nin conjugated to horseradish peroxidase. **A:** The deposit was in the rostral, low-frequency (Knight, 1977) part of the anterior auditory field. **B:** The injections did not reach the anterior ectosylvian gyrus or the suprasylvian fringe cortex (SF; see Fig. 1A). **C:** Independent foci of labeling extended caudorostrally through the auditory thalamus. **D:** Parallel bands of transport remained in register as they crossed the boundary between the ventral (V) and medial (M) divisions.

E: Both divisions had significant zones of anterograde nonreciprocity, although the projections were largely reciprocal (Fig. 15A). **F:** The breadth of ventral division (V) labeling included much of both *pars lateralis* and *pars ovoidea*. **G:** Labeling in the dorsal nucleus (D) increased in density rostrally. **H:** In the rostral pole, some foci were independent and nonreciprocal. Protocol as in Figure 3. See Figure 5 for comparison with biotinylated dextran amines-labeled boutons from a similar experiment.
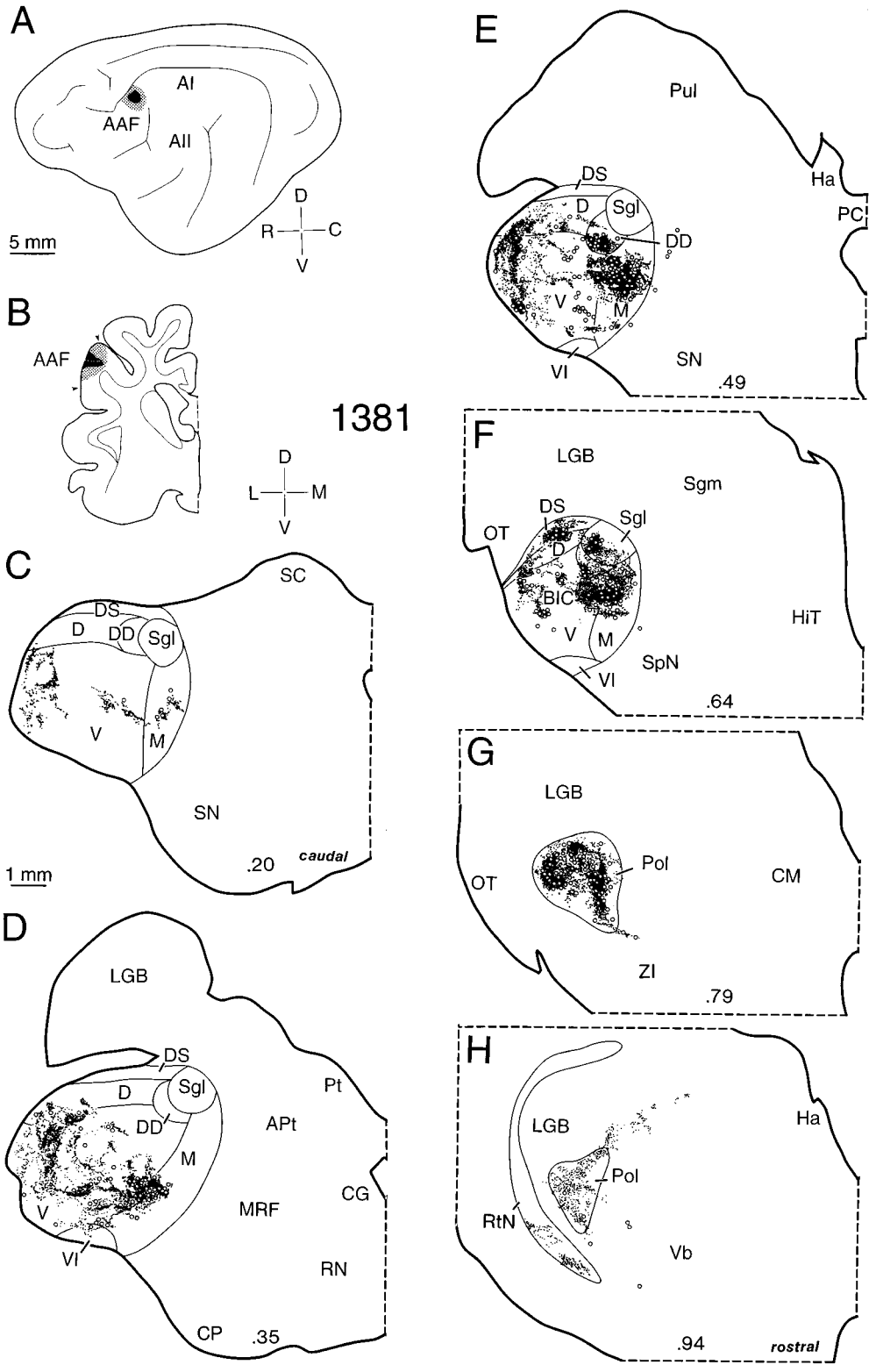
Figure 5

ing, anterograde CT terminals, were found in the medial division (Fig. 4C: M) and clouds of fine anterograde labeling extended into the dorsal nucleus (Fig. 4C: D). In the next section, these single foci coalesced into one mass in all but a few instances (Fig. 4D), and these projections extended more strongly into the medial division than in the AI experiment (Fig. 3D: M). The labeling reached, but did not enter, the ventrolateral nucleus (Fig. 4D–F: Vl), which is a displaced part of the dorsal division and a target of nonprimary cortical areas; these data are summarized in Figure 15A: Vl. In the next section (Fig. 4E), the projection reached its peak and retained most of the features from more caudal levels. The transport was still patchy, there were significant zones of both anterograde and retrograde nonreciprocity (especially in the medial division), the ventrolateral nucleus had little or no input, and the projection avoided the most rostral (low frequency) part of AAF, in agreement with physiologic estimates of its boundaries (Knight, 1977). The labeling was more focal and discontinuous in more rostral sections (Fig. 4F). The dorsoventral orientation of transport in the lateral part of the ventral division was consistent with the fibrodendritic lamination pattern (Morest, 1964), as was the more complex arrangement in the *pars ovoidea*, where the laminae may rotate up to 90 degrees, and the physiologic organization is modified correspondingly (Imig and Morel, 1984). A small but consistent projection to the dorsal nucleus (Fig. 4F: D) continued rostrally (Fig. 4G). Another new trend emerged that will be repeated in subsequent experiments: the lateral nucleus of the posterior group (Pol), which began at ≈0.75% of the caudorostral length (Fig. 4H) and represents much of the rostral pole of the medial geniculate body, had a pattern of input that is unique among auditory thalamic nuclei. Projections to it are highly focal and patchy (for example, Fig. 6H: Pol) in some cases, or primarily anterograde in others (Fig. 5H: Pol), and virtually absent in certain experiments (Figs. 9G,H, 10H). The present experiment illustrates this complexity, if on a reduced scale. The robust terminal labeling in the thalamic reticular nucleus was plotted in the BDA experiment (Fig. 5H: RtN). It was omitted from the corresponding WGA-HRP experiment (Fig. 4), because the many fascicles of labeled thalamocortical and corticothalamic axons reduce the reliability of charting terminals in these preparations.

On a global basis, the results from the WGA-HRP deposits (Fig. 4) and from analogous BDA injections (Fig. 5) were similar. The chief difference between them was the

BDA labeling in the lateral part of the suprageniculate nucleus and its absence in this WGA-HRP experiment. Whether this finding is a reflection of slight differences in the intra-areal position of the deposits (Figs. 4B, 5B) or possible encroachment of one of the deposits on an adjoining subregion, is unknown.

Area P. The unusually rostral position of the posterior ectosylvian gyrus (Fig. 1A: pes) in this experiment (Fig. 6A) complicated the interpretation of this injection site. The deposits were made on the caudal face of the gyral bank (Fig. 6B) and did not appear to reach the AI border, which was ≈2 mm dorsal. However, the cytoarchitectonic distortion made an exact determination of the boundaries difficult. The deposits reached layer VI; the cortex beneath the injections was the posterior face of the ectosylvian gyrus. The deposit was ≈5 mm high and 2 mm long, with little invasion of the white matter.

The features shared with the prior experiments include evidence for a topographic relation with respect to the site of deposit, discontinuous patches of labeling (Fig. 6E), regions of significant nonreciprocity (Fig. 6D: V, 6E: Ov), and substantial involvement of the lateral part of the posterior group (Fig. 6H: Pol). A unique feature was the many retrogradely labeled neurons, without a corresponding CT projection, especially in the medial division.

Substantial labeling was present in the caudal part of the ventral division (Fig. 6C) and it included both CT terminals and TC neurons in close proximity. A small but substantial focus of transport in the *pars ovoidea* (Fig. 6C–D) confirms that most of the deposit was in area P, and the labeling had a dorsal, low-frequency to ventral, high-frequency, progression consistent with the arrangement reported in electrophysiologic studies (Reale and Imig, 1980). The substantial involvement of the *pars ovoidea* would seem certainly to exclude AI and possibly to eliminate the ventral posterior (VP) auditory field as alternative candidates because their high frequency domains were remote from the injection site. The ventrolateral nucleus was largely spared, indicating that the posterior ectosylvian gyrus was not involved significantly.

Differences from the prior experiments were the pronounced retrograde nonreciprocity, especially in the medial division (Fig. 6D,E: M), and the highly focal projections (Fig. 6D: D; 6H: Pol) in which zones of more or less complete reciprocity lay near strongly nonreciprocal regions. A further distinction was the massive involvement of the medial division, including subareas where thalamocortical projections predominated (Fig. 6C–E: M) or CT

Fig. 5. Connections from area AAF by using biotinylated dextran amines (BDA). **A:** The deposit core was ≈1.5 mm in diameter, with a halo of diffusion. The deposit was confined to AAF and was approximately half the size of that in the wheat germ agglutinin conjugated to horseradish peroxidase (WGA-HRP) experiment (Fig. 4A). **B:** Tracer filled the crest of the anterior suprasylvian gyrus, and the diffusion did not reach the white matter. **C:** Scattered foci of light labeling were present. There were few terminals and no obvious boutons de passage. Preterminal processes were omitted. **D:** The long vertical mass of labeling in the ventral division suggests that isofrequency laminae in AAF had an orientation comparable to those in AI (see Fig. 4D; Knight, 1977). **E:** The dorsal division foci of labeling probably reflect the incursion into the overlying suprasylvian fringe cortex (B), although the rostral extent of this field is unknown. Retrogradely labeled neurons without a reciprocal corticothalamic pro-

jection were present in the central part of the ventral division. Medial division (M) labeling was among the most intense in the series, and it was heavier than that in the WGA-HRP experiment. **F:** Sheets of heavy labeling filled much of the superficial dorsal nucleus (DS), and the lateral part of the suprageniculate nucleus (Sgl) was also a prominent target. **G:** Input to the rostral pole (Pol) was intense, mixed, and unusually focal; this was one of the largest projections to this nucleus. Wisps of fine labeling extended into the posterior intralaminar territories beneath the medial geniculate body. **H:** This section captures the sensitivity of the method, showing small patches of terminals dorsomedially in the central part of the thalamic intralaminar system, and robust patches of terminals in the appropriate part of the thalamic reticular nucleus (Crabtree, 1998). The strong reciprocal projections in Pol were unusual; this was the most anterior auditory thalamic section in this study with significant input.
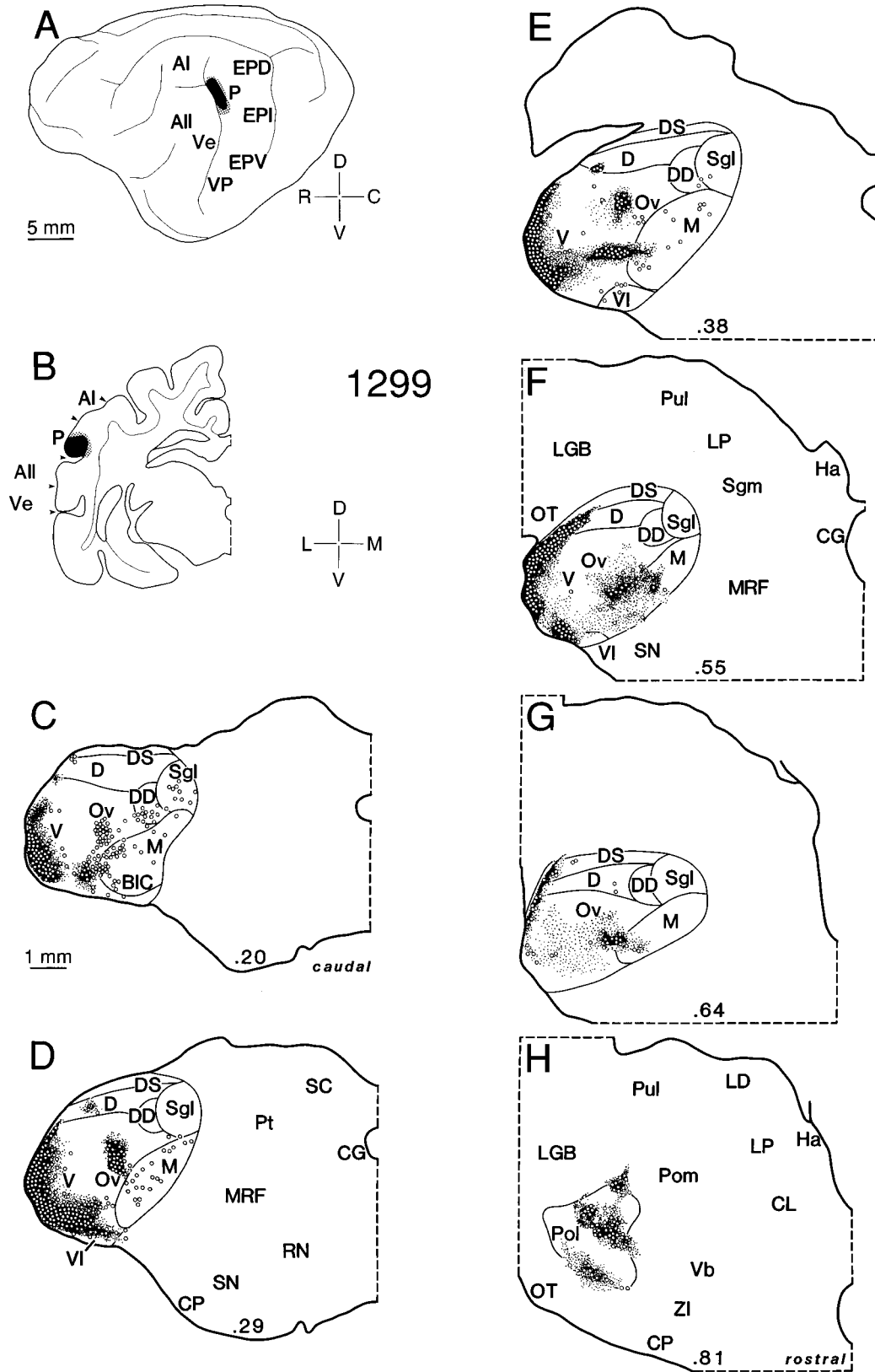
Fig. 6. Connections of area P. **A:** The injections saturated the dorsal half of this field. **B:** The injection spread dorsally to within ≈1.5 mm of area AI, and it was ≈3 mm from the border with the ventral posterior auditory field (VP). **C:** Areas of nonreciprocity were marked in the dorsal and the ventral divisions. **D:** The medial division projection was entirely retrograde. **E:** A small cluster of mixed labeling was present at the most lateral part of the dorsal nucleus (D); this focus was present in subsequent sections (C–G). The massive, continuous projection to the ventral division (V) extended ≈2 mm and reached the medial division border (M). **F:** The labeling in *pars* *ovoidea* (Ov) and in the medial division (M) became progressively anterograde, and in the *pars lateralis* (V) it was mixed. **G:** Clustered labeling in the dorsal nucleus (D) appeared more rostrally as a sheet, while the input to the medial division (M) caudally (panel F) began to decline. Scattered, retrogradely labeled neurons were present in the dorsal division. **H:** The rostral pole (Pol) had a new pattern of projection, in which both the ventral (panel C) and lateral (panel E) distributions were replaced by a triple input whose parallel sheets crossed Pol obliquely, from dorsolateral to ventromedial.

axons were numerous (Fig. 6F,G: M). The labeling in Pol (Fig. 6H) confirmed the complex, periodic topography of this projection and resembled the foci of transport in the subdivisions of the ventral nucleus (Fig. 6D–F: V,Ov).

In two further experiments using BDA (not illustrated), much the same distribution and similar foci of labeling were found in these thalamic nuclei. The continuity of CT labeling within the tonotopically organized fields (Fig. 14) suggests that these projection patterns were shared by remote regions with similar functional affiliations (Winer, 1992).

Area AII. This experiment differed from the preceding ones by labeling principally dorsal division nuclei, by its more complex projection pattern, in having more nonreciprocal projections, and in the reduced medial division labeling (Fig. 7). Parallels included topographic relationships between the injection site and the thalamic labeling even when the injected area has little tonotopic representation (Schreiner and Cynader, 1984).

The injections were in the central part of the second auditory cortex (area AII), ≈4 mm equidistant from the AI border (Fig. 7A) and from the insular cortex (Fig. 7A: Ins) borders. The deposits reached layer VI, <2 mm beneath the cortical surface; the deeper cortex was the bank of the peri-insular area abutting the pseudosylvian sulcus (Fig. 1A: pes). Although some connections were shared with insular cortex (Fig. 15A: Ins,AII), the patterns were sufficiently distinct to conclude that the AII deposits were limited to this area (compare Figs. 7, 9).

The ensuing labeling involved many dorsal division nuclei (Fig. 14: AII). Input to the ventral division was sparse, diffuse, and mixed. The ventral division proper was defined more by exclusion than by the intensity of labeling (Fig. 7C). Except in the *pars ovoidea* (Fig. 7D: Ov), where there were foci of input, most of the projection ended in the dorsal and the deep dorsal nuclei and the lateral part of the suprageniculate nucleus (Fig. 7D: D,DD). This was the only experiment with significant marginal zone labeling (Fig. 7F: MZ), and it was almost entirely anterograde. The caudal dorsal nucleus (Figs. 2A, 7C: DCa) had a heavy projection with interdigitated areas of reciprocal or patchy input; the regions of focal projection contained only one type of labeling. There was a similar pattern in the dorsal nucleus (Fig. 7D: D), although the projection was more discrete than elsewhere in the dorsal division. The characteristic AII distribution was present even in single sections: the lateral part of the superficial dorsal nucleus (Fig. 7E: DS) received only anterograde labeling; the dorsal nucleus (Fig. 7E: D) had reciprocal connections; the suprageniculate nucleus (lateral part) contained mainly cells of origin (Fig. 7E: Sgl), much like the medial division; and the ventrolateral nucleus (Fig. 7E: Vl) had many thalamocortical neurons and few CT axons; whereas the ventral division received little input (Fig. 7E: V, Ov).

In this (Fig. 7E) and subsequent sections, a new pattern emerged in the medial division (Fig. 7F: M). At caudal levels (Fig. 7C,D: M), the labeling was mainly retrograde, and restricted largely to the border abutting the *pars ovoidea*; it was now far heavier, mixed, and invaded the center of this division. Rostrally, it ended abruptly (Fig. 7G: M). A second pattern emerged that will be repeated in other experiments: there was a complex arrangement of input to the lateral part of the posterior group (Fig. 7H: Pol), which had an orderly mediolateral orientation with

independent bands of transport, as in several other cases (Figs. 6H, 8H: Pol).

In two further experiments (not shown), the deposits and the locus of thalamic labeling were virtually identical to those in the case illustrated. The confirmatory studies used WGA-HRP or BDA.

Area EP. Three cases are reported that involve tracer injections in the posterior ectosylvian gyrus (Fig. 1A: EPI/EPD). These deposits produced the most divergent projections in our survey, labeling up to 15 auditory and visual nuclei in the thalamus. Because the cytoarchitectonic borders in this periauditory region and its physiological organization have not been established definitively (Bowman and Olson, 1988a,b), it was divided into three territories (dorsal, intermediate, and ventral) to characterize its thalamic relations.

The first case (Fig. 8) was a WGA-HRP injection centered in the intermediate part of the gyrus and slightly posterior to its midpoint; it is referred to as EPI. The deposit was ≈4 mm high and 3 mm in diameter and was restricted to the gray matter with minimal subcortical diffusion (Fig. 8B). The principal result was that all dorsal division nuclei were labeled to one degree or another. Some, like the ventrolateral nucleus (Fig. 8D–F: Vl) had only meager input, whereas the medial part of the suprageniculate nucleus had much heavier projections (Fig. 8E: Sgm). This is in accord with the perivisual affiliations of this cortical area (Bowman and Olson, 1988a) and this nucleus (Benedek et al., 1997). The medial division had intense and reciprocal transport in one section (Fig. 8C: M) and predominantly retrograde labeling elsewhere (Fig. 8D: M).

The dorsal superficial nucleus, particularly its dorsolateral sector, was labeled densely with CT terminals in some sections (Fig. 8C: DS) and had many retrogradely labeled cells in others (Fig. 8D,E). The transport diminished abruptly at the ventral division border (Fig. 8D: V) and filled the entire dorsal superficial nucleus in caudal sections (Fig. 8C: DS). More rostrally, the labeling moved medially (Fig. 8F: DS). In contrast, the entire lateral subdivision of the suprageniculate nucleus was labeled strongly (Fig. 8C–E), except at its rostral pole. The medial part of the suprageniculate nucleus was largely defined by the mixed labeling along its caudorostral extent (Fig. 8E–G: Sgm), and scattered foci of CT input entered the mesodiencephalic reticular formation (Fig. 8C: MRF) and the pulvinar nucleus (Fig. 8G: Pul), which also had retrogradely labeled neurons.

Medial division input was distributed uniquely. Caudally, only cells were labeled (Fig. 8D: M), whereas rostrally there were mainly CT terminals (Fig. 8F: M); intermediate sections had mixed labeling (Fig. 8E: M). This pattern was incompatible with the idea that medial division cortical connections are homogeneous or nonspecific (Winer and Morest, 1983a). The input to the lateral part of the posterior nucleus was also unusual: caudally, it formed a continuous band whose most lateral part was entirely anterograde and whose medial two-thirds was mixed (Fig. 8G), whereas more rostral sections also had mixed input situated more centrally (Fig. 8H). There was a focal projection in Pol as in some (Fig. 6H: Pol) but not all (Fig. 3H: Pol) of the prior experiments. Scattered, labeled neurons extended into the region between the zona incerta and the inferior face of the ventrobasal complex (Fig. 8H), an area identified in cats and marsupials as a
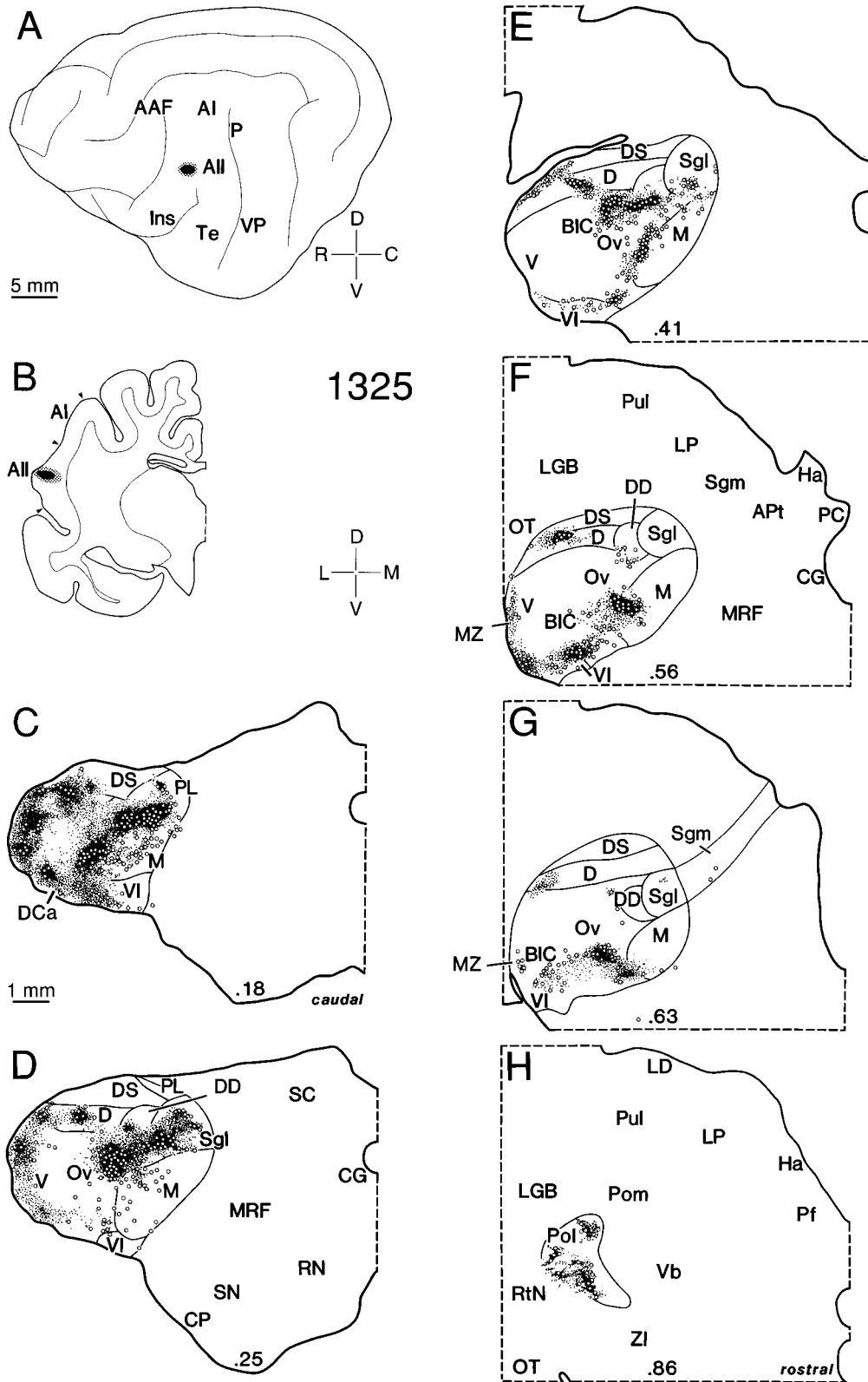
Fig. 7. Connections of area AII. A: The deposits were in central AII, between the posterior and anterior ectosylvian sulci, and above the pseudosylvian sulcus (Fig. 1A). **B:** The injection was ≈1.5 mm wide and reached the white matter. The tissue beneath the deposits represents buried, pseudosylvian cortex. **C:** This was the heaviest terminal labeling and the near-maximum concentration of cells of origin in the experiment, with at least six independent foci. **D:** There were several nonreciprocal projections, including terminals without cells in the ventral division (V) and cells without terminals in the medial division (M). Labeling was nearly as focal as in panel C. **E:** The most lateral part of the intersection of the superficial dorsal (DS) and dorsal (D) nuclei contained a small subregion with mixed labeling, including a dense concentration of terminals (see the Discussion sec-

tion). In biotinylated dextran amines (BDA) experiments, many endings here were unusually large (Winer et al., 1999). **F:** Except in the ventrolateral nucleus (Vl), which was labeled completely, all other input was patchy and topographic. The deep dorsal nucleus (DD) had only retrogradely labeled neurons in this section, mixed labeling elsewhere (E), and no projections in other sections (G); this finding suggests intranuclear differences in the homogeneity of input. **G:** The smaller projections to dorsal division nuclei were usually discrete puffs of anterograde, retrograde, or mixed transport, often near nuclear borders. **H:** Connectional diversity occurred in the lateral part of the posterior nucleus (Pol), where anterograde labeling dorsomedially was separated from a band dominated by terminals in the ventral and lateral part.
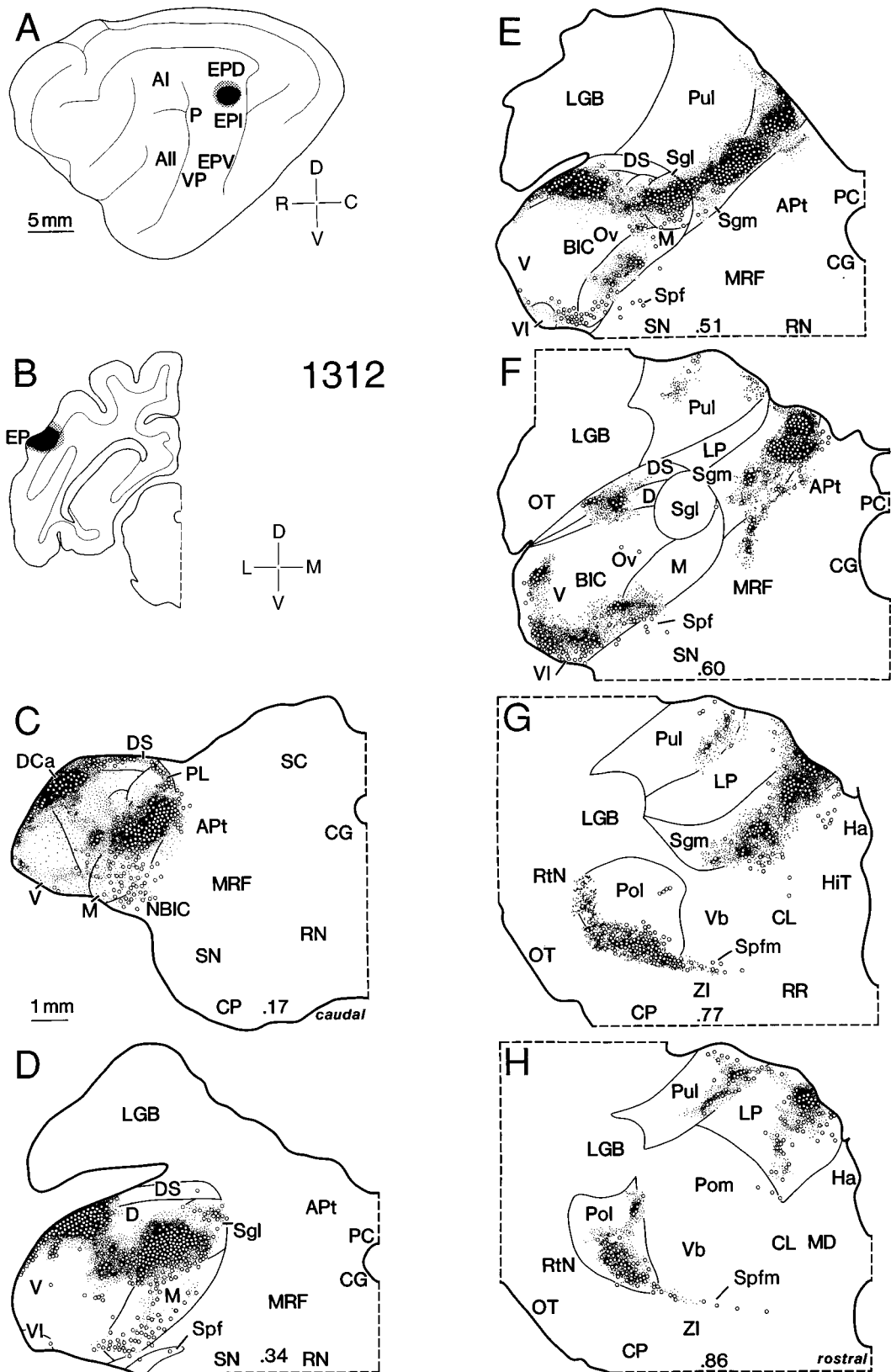
Fig. 8. Connections of area EPI. **A:** The deposits were in regions whose borders have not been described in the same detail as those of the primary fields. **B:** The injections filled ≈7 mm² of the posterior ectosylvian gyrus. **C:** The labeling was variable in some nuclei, such that the lateral part of the dorsal division received a heavy and mixed projection, whereas cells of origin dominated more medially (DS). **D:** The deep dorsal nucleus (not denoted; see Fig. 2C: DD) and adjoining dorsal division nuclei were labeled intensely. **E:** The medial division (M) had some of the strongest input in this series (see Fig. 15A: EPI), and it was variable (compare panels D,F). Most dorsal division nuclei were filled with labeling or had none. **F:** The ventral division (V) labeling was unexpected (Winer et al., 1977), whereas the pulvinar (Pul) and suprageniculate (Sgm) projections were (Bowman and Olson, 1988b). Perhaps some thalamic axons en route to AI were damaged (Fig. 8B). **G:** The mixed labeling in the lateral part of the posterior nucleus (Pol) may link it with the ventral division (panel F: V). **H:** The labeling in this experiment extended farther rostrally than in all but two other cases (Figs. 7, 9). Small but consistent connections with the subparafascicular nucleus (Spf) in the posterior intralaminar system (Winer et al., 1988) were a feature of this and other experiments involving nonprimary areas (Figs. 9,10).

medial extension of the posterior intralaminar thalamic system (Winer et al., 1988). The multisensory affiliations of EPI/EPD were confirmed by its connections with both the pulvinar and the lateral posterior nucleus, each of which had abundant, mixed transport (Fig. 8G: Pul, LP).

A second case (not illustrated) is summarized in Figure 14 (EPD); it involved a deposit of WGA-HRP dorsal and rostral to the EPI experiment, and caudal to AI, just behind the posterior ectosylvian sulcus (Fig. 1B: open black circle on posterior ectosylvian gyrus). It had more labeling in the ventral division, particularly in the *pars ovoidea* (Ov), and heavy projections to the caudal dorsal division (DCa) and the pulvinar nucleus (Pul), but otherwise resembled the EPI case (Fig. 14).

In a third experiment (not shown), BDA was injected in EPD, slightly caudal to the preceding deposit (Fig. 1B: open white circle on posterior ectosylvian gyrus), and possibly encroaching onto the secondary visual areas of this gyrus (Tusa et al., 1981). For convenience only, we have designated the case posterior ectosylvian gyrus, posterior part (Fig. 14: EPP). The labeling involved mainly the dorsal division and included the superficial dorsal nucleus, both parts of the suprageniculate nucleus, and the pulvinar and lateral posterior nuclei. It contrasted sharply with the EPI case illustrated in producing no labeling in the inferior colliculus (Fig. 14) nor in the caudal dorsal nucleus of the medial geniculate body (Fig. 14). This finding suggests that several fields might exist in the posterior ectosylvian gyrus, each with a distinct auditory affiliation.

Area Ins. The insular (Ins) cortex injection (Fig. 9) and the next experiment on temporal cortex (Te; Fig. 10) shared many features (Fig. 15A: Ins, Te). Both had more restricted corticothalamic-thalamocortical connections than areas AII, EPI, and EPV, and more such projections than areas AI, AAF, P, and VP. Second, their involvement with Pol was minimal, suggesting that limbic related nonprimary cortex operates independently of the rostral pole, and that this nucleus has ascending input mainly to primary and polysensory cortex (Fig. 15A).

Two experiments had injections confined to the anterior sylvian sulcus, in the auditory subregion of the insular cortex (Clascá et al., 1997). One case (illustrated) involved the ventral bank and used WGA-HRP, whereas the other was more dorsal and used BDA. In both, the labeling pattern was similar.

The deposit was 4 mm tall and centered in the rostral bank of the pseudosylvian sulcus (Figs. 1A: ps; 1B: 9, 9A). The injection spread slightly into the claustrocortex but did not invade the claustrum. Although the tracer extended dorsally, it was far from area AII and it did not cross the fundus of the pseudosylvian sulcus.

The principal thalamic target was both parts of the suprageniculate nucleus through most of their extent (Figs. 9C–H; 11B: Sgl, Sgm). The lateral part had many CT terminals and neurons in close proximity. Scattered terminals and foci of neurons were also in the dorsal caudal nucleus (Fig. 9C: DCa) and in the subparafascicular and suprapeduncular nuclei (Fig. 9C: Spf, SpN). More rostrally, these nuclei had only labeled neurons (Fig. 9D), which were part of a larger projection that included the lateral mesencephalic nucleus (Fig. 9C,D: LMN). A few labeled cells and sparse terminal fields were found in the substantia nigra; the terminals were restricted to the *pars reticulata* (Fig. 9C: SNr).

Besides the substantial suprageniculate nucleus connections, the deep dorsal nucleus was filled with axon terminals and neurons in its caudal two-thirds (Fig. 9D–F). Such a projection did not target all dorsal division nuclei because the superficial dorsal (Fig. 9D: DS) and dorsal nuclei (Fig. 9F: D) were largely spared; this was one of the few experiments in which the lateral part of the dorsal superficial and dorsal nuclei was without labeling (see Figs. 6F, 7C, 8D). The ventrolateral nucleus was also free of transport caudally (Fig. 9D: Vl) and had labeled cells rostrally (Fig. 9G: Vl).

The medial division likewise had significant projections, although the type and density was variable. Often, only the dorsal half was involved, and the projection was heavy and mixed (Fig. 9C). Although this finding might be considered as an extension of the dense input to the suprageniculate nucleus, it was present sometimes in the latter (Fig. 9G: Sgm) and not in the former (Fig. 9G: M).

Other limbic affiliated regions also had labeling, including weak CT projections to the habenula (Fig. 9F: Ha) and to the central gray (Fig. 9F: CG), stronger input to the medial dorsal thalamic nucleus (Fig. 9H: MD), mixed projections to the medial dorsal nucleus (Fig. 9G: MD) along its medial border, and labeled cells scattered in several hypothalamic areas (Fig. 9H: HDA,HPA; Fig. 10G: LHA). Many labeled neurons were found in the subthalamic nucleus as well (Fig. 9G: St).

Area Te. These experiments demonstrated the connectional independence of temporal (Fig. 1A: Te) and insular cortical areas. The medial limb of the suprageniculate nucleus was significantly involved with insular (Fig. 9: Sgm), but not with temporal (Fig. 10: Sgm), cortex.

Two cases (one WGA-HRP, one BDA) received injections confined to the temporal gyrus, ventral to area AII and caudal and inferior to area Ins. The WGA-HRP experiment was chosen for illustration and the distribution of labeling was identical except for the involvement of the subparafascicular nucleus in the BDA experiment.

The deposit was oval and ≈5 mm in diameter (Fig. 1B: 10); it reached, but did not invade, the pseudosylvian sulcus (Fig. 1A: ps) and it filled the ventral bank of the posterior ectosylvian sulcus (Fig. 1A: pes); it saturated the gray matter (Fig. 11B) without entering area AII. There was massive, mixed input to several parts of the dorsal division, including the caudal dorsal (Fig. 10C: DCa; Fig. 11D: DCa), dorsal superficial (Fig. 10D: DS), dorsal (Fig. 10E: D), and ventrolateral (Fig. 10E: Vl) nuclei. Although the lateral part of the suprageniculate nucleus contained significant labeling, it differed in two ways from other dorsal division labeling. First, the caudal part of the nucleus had only CT input (Fig. 10C,D: Sgl). Second, in more rostral sections the projection was mixed, focal, and far weaker (Fig. 10E–G: Sgl), and the same pattern was present in the medial part of the suprageniculate nucleus (Fig. 10G: Sgm). Given the size of this deposit relative to others (Fig. 1B), these differences may not reflect incomplete injection of a field. The deep dorsal nucleus was packed with mixed labeling, such that the CT terminals alone defined the caudal suprageniculate nucleus (Fig. 10D: Sgl), and heavier mixed labeling lay nearby. Other dorsal division nuclei, especially the superficial dorsal (Fig. 10E: DS), dorsal (Fig. 10D: D), and ventrolateral nuclei (Fig. 10E: Vl), had far more input than in the insular cortex experiment (Fig. 9). The medial division labeling was heavy through much of its length, and con-
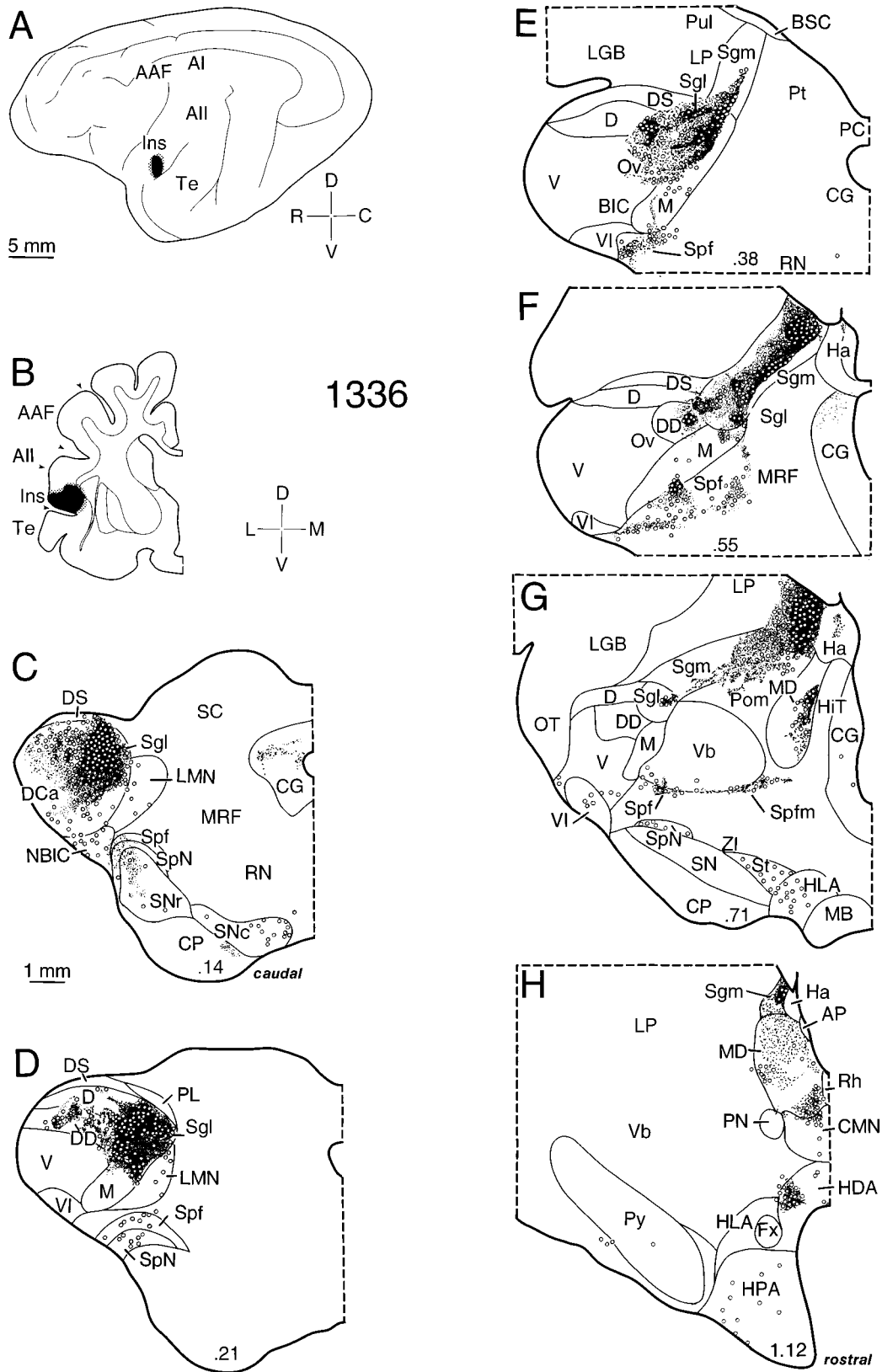
Fig. 9. Connections of area Ins. **A:** The deposit was confined to insular cortex. **B:** The injections filled much of the insula and encroached onto the extreme capsule. **C:** Nearly all of both parts of the suprageniculate nucleus (Sgl, Sgm) were labeled through their caudorostral extent. **D:** There were few terminals in the dorsolateral part of the dorsal division (see Figs. 6–8, 10: DS,D). **E:** The projections were patchy, with foci dominated by one type of input. The medial division (M), for example, had a complex, section-specific labeling pattern. **F:** The subparafascicular nucleus (Spf) had robust cortical projections, with little CT input, whereas the central gray (CG) had exclusively corticofugal projections in this section and some projection neurons rostrally (panel G). The ventral division was spared almost entirely. **G:** This and the next section showed the powerful, limbic-related subcortical connections of insular cortex. The medial part of the posterior group (Pom) had only thalamocortical labeling, as did the lateral hypothalamus (LHA), whereas projections in the central medial nucleus (CMN; panel H) were mixed. **H:** This was the only experiment with strong labeling rostral to the medial geniculate body, and it was one of just three cases with no connections to the lateral part of the posterior group (Fig. 15A: Pol).
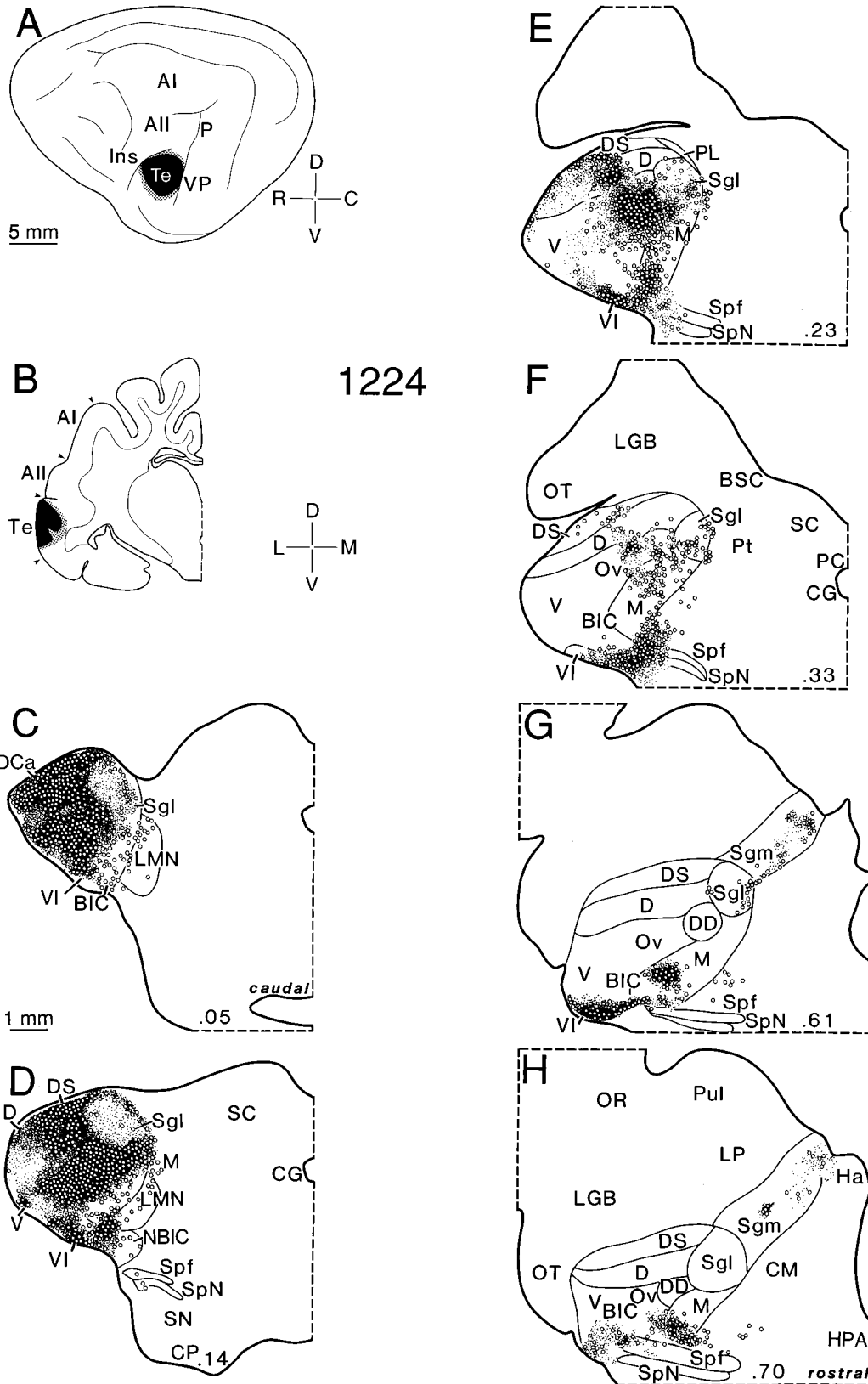
Fig. 10. Connections of area Te. **A:** The deposits were centered in temporal cortex, except caudally, where the ventral auditory field may have been involved (see panel D: V). **B:** The piriform cortex ventral to area Te was not involved. **C:** This experiment revealed connections with the caudal dorsal nucleus (DCa) that were among the strongest and most extensive in this series. It alone labeled extrageniculate neurons in the lateral mesencephalic nucleus (LMN). **D:** The medial division (M) retrograde labeling in this and in subsequent sections (E,F) was also unusually strong; CT projections were largely absent. **E:** The intralaminar nuclei (Spf, subparafascicular; SpN, suprapeduncular) were involved variably along much of their caudorostral extent, although the extensive rostromedial intralaminar labeling in other experiments (Fig. 9: Spf,SpN) was absent here. **F:** Retrograde labeling predominated rostrally, with focal projections from many dorsal division nuclei. **G:** This marked substantial involvement of the medial division (M) rostrally and suggested that anterior dorsal division territories were related more closely to areas AII (Fig. 7G) and EP (Fig. 8F). **H:** Despite the massive injection, the suprageniculate nuclei (Sgl, Sgm) were labeled lightly, especially Sgm, and these projections were focal rather than continuous as in the insular cortex experiments (Fig. 9F).
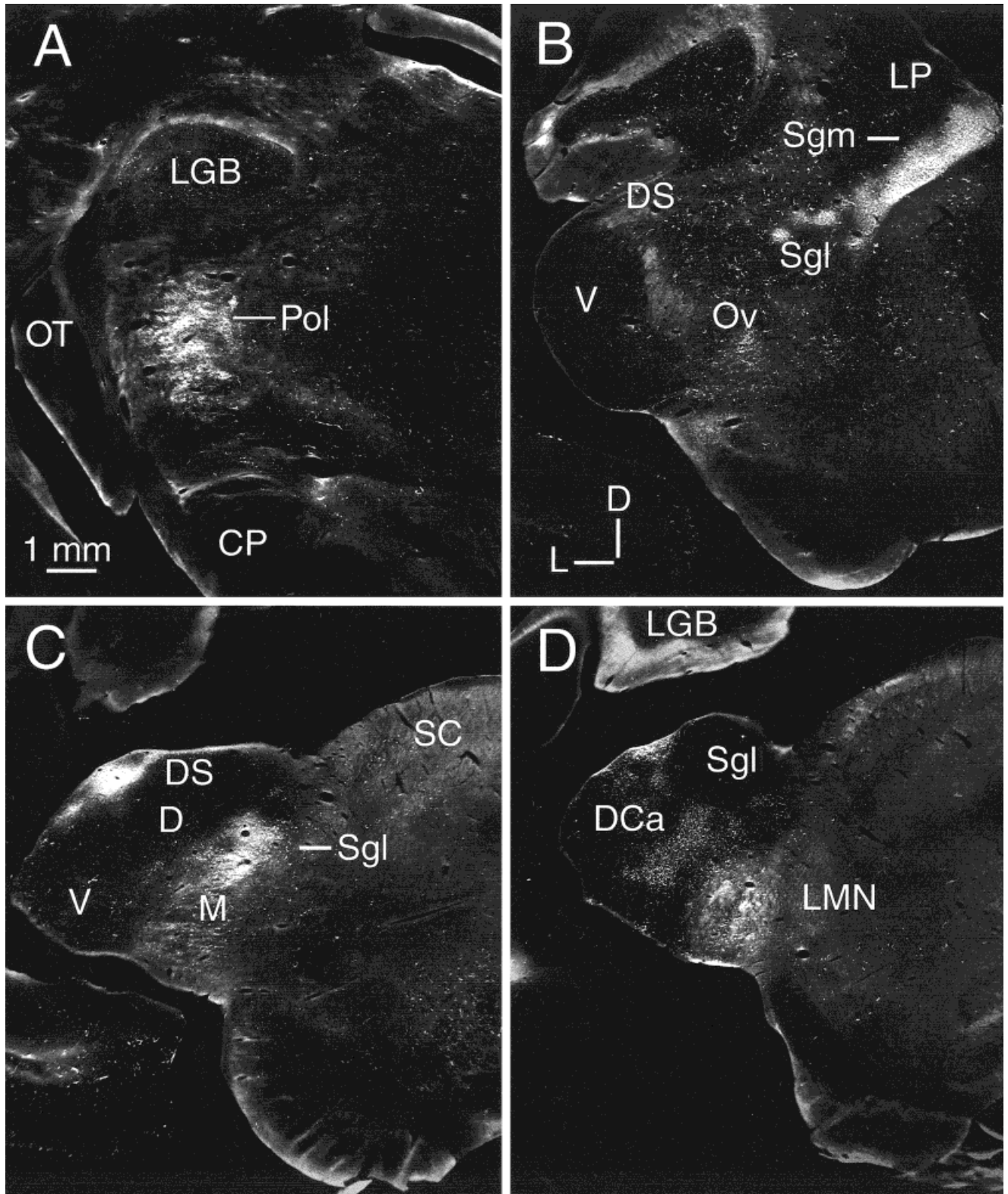
Fig. 11. Representative examples of auditory thalamic labeling. **A:** Mixed input fills much of the lateral part of the posterior nucleus (Pol; Fig. 3H) from an AI injection (Fig. 3A). Axon terminals and retrogradely labeled neurons were intermingled. Protocol for A–D: Planachromat, N.A. 0.04, ×12.5. Darklight™ darkfield condenser (Micro Video Instruments, Inc., Avon, MA). Details on digital processing appear in the legend to Figure 1. **B:** Mixed projections in the medial part of the suprageniculate nucleus (Sgm; Fig. 9F) after insular cortex deposits (Fig. 9A). The heavy labeling filled the central part of the nucleus and extended laterally into other dorsal division nuclei. **C:** Labeling in the superficial dorsal (DD; Fig. 8D) and in the lateral part of the suprageniculate nucleus (Sgl) after deposits in the intermediate part of the posterior ectosylvian gyrus (Fig. 1B, below #8). Moderate anterograde labeling in the intervening dorsal division nuclei links the two massive clusters. **D:** Connections of the caudal dorsal nucleus (DCa; Fig. 10C) and adjacent nuclei after temporal cortex deposits (Fig. 10A: Te). Much of the fine terminal labeling in DCa was not visible at low power.

sisted mainly of thalamocortical neurons caudally (Fig. 10C–F: M) and more mixed input rostrally (Fig. 10G,H: M). There were scattered neurons labeled in the lateral mesencephalic nucleus (Fig. 10D: LMN) and appreciable mixed projections in the ventrolateral and the posterior intralaminar thalamic nuclei (Fig. 10F,G: Vl,Spf,SpN) and adjoining territories. The absence of projections to limbic-related nuclei (Fig. 10G,H) contrasted with the results of the insular experiment (Fig. 9F–H).

Deposits in other fields

For purposes of economy and inclusiveness, the results from experiments in which other, architectonically defined auditory cortical regions were injected are described briefly and not illustrated. The ensuing distribution of labeling was sufficiently similar to one of the other projection patterns described above that a separate, equally detailed treatment is unnecessary.

Area VP.   This BDA experiment had an injection in the ventral part of the posterior ectosylvian gyrus, along its rostral face (Fig. 1B: triangle). The locus and density of thalamic labeling were similar to those after deposits in AI (Fig. 3), AAF (Fig. 4), and area P (Fig. 6; see also Fig. 15A).

Area Ve.   This case had a highly circumscribed WGA-HRP deposit centered in the rostral bank of the posterior ectosylvian sulcus, just inferior to the caudal, low-frequency part of AI (Fig. 1B: asterisk). The labeling in the auditory thalamus was similar in location and intensity to that in all other experiments that involved primary auditory fields (Fig. 14A), areas whose topographic arrangement of characteristic frequency has been documented in physiological studies (Reale and Imig, 1980).

Area SF.   In two further experiments, the cortex along the crest of the middle ectosylvian gyrus, above area AI and lateral to the visual association areas along the bank of this gyrus (Tusa et al., 1981), was injected with WGA-HRP (Fig. 1B: star). In one case, both AI and the more medial perivisual areas were spared entirely and the pattern of transport was similar to that from areas AII (Fig. 7), Ins (Fig. 9), EPI (Fig. 8), and Te (Figs. 10, 15A). This confirmed its relation to nonprimary, nontonotopic cortical fields (Winer, 1992).

DISCUSSION

Implications for cytoarchitecture

The present results are germane to issues of architectonic parcellation, both in the cortex and in the thalamus. In the posterior ectosylvian gyrus, for example, it has been proposed that the caudal regions have the strongest visual affiliations, whereas progressively rostral territories are more closely related to the auditory system (Bowman and Olson, 1988a,b). The present results, although consistent with such an assignment, suggest that even the caudal half of the dorsal part of the posterior ectosylvian gyrus has significant connections with the principal nuclei in the medial geniculate body as well as nonauditory thalamic regions (Fig. 8) and significant input to the rostral pole of the medial geniculate body (Pol). A more complete physiological analysis, correlated with patterns of connectivity, would be instrumental in establishing such boundaries.

A similar argument can be made with regard to particular thalamic nuclei. For example, a small territory in the

dorsolateral margin of the dorsal division, which has not, to our knowledge, been recognized as a discrete nucleus on either architectonic (Morest, 1964, 1965) or connectional (Winer et al., 1977) grounds, was labeled consistently by deposits in areas AAF (Fig. 5D), P (Fig. 6D,E), AII (Fig. 7E), EPD (Fig. 8D), and Te (Fig. 10E), but not after insular cortex injections (Fig. 9). This region was not identified as a distinct nucleus on physiological (Imig and Morel, 1984, 1985) or on architectonic criteria (Rose and Woolsey, 1949; present results) or on the basis of its neuronal architecture (Winer and Morest, 1983a,b, 1984). The breadth and complexity of its cortical connections suggest that this dorsolateral subdivision of the dorsal nucleus could integrate primary and nonprimary streams of information traversing the thalamus. The lack of physiological data constrains more explicit hypotheses.

Status of the lateral part of the posterior group

The rostral one-quarter of the medial geniculate body (PO, Pol) is largely refractory to Golgi impregnation (Winer, 1992) because of its heavy myelination (Fig. 2H). It is situated between the lateral geniculate body, the thalamic reticular nucleus, the posterior intralaminar complex, and the ventrobasal thalamic nuclei, each of whose intricate myeloarchitecture complicates the interpretation of this region of the thalamus. Its neuronal composition has not been described in detail except in Nissl preparations, where it was designated as PO (Imig and Morel, 1985). However, it is auditory on the basis of ascending input from the inferior colliculus (Andersen et al., 1980b) and by virtue of its descending projections from AI and AII (Andersen et al., 1980a) and five other auditory cortical areas (Fig. 14). In electrophysiological studies, the tonotopic organization of PO was described as consisting of irregularly shaped slabs oriented mediolaterally and across which higher frequencies (≥ 16 kHz) are arrayed in the most caudal block, whereas lower frequencies (≤ 2 kHz) are most rostral; intervening best frequencies ($4-8$ kHz) are located in an intermediate slab. These slabs, then, are independent of the representation of best frequency in the more caudal part of the ventral division, and they form a medial-to-lateral sequence in the rostral pole that contrasts with the complex geometry of tonotopic representation of middle- and high-frequency maps more caudally (Imig and Morel, 1985, p. 845). Other physiological data suggests close parallels between the ventral division proper and Pol with regard to the proportions of azimuth-sensitive/insensitive monotonic and nonmonotonic neuronal populations (Barone et al., 1996).

Our data suggest that PO/Pol is certainly a part of the medial geniculate body, receiving input from up to eleven auditory cortical fields (Fig. 14). However, some of its neurons project to SII (Bentivoglio et al., 1983), so that certain elements of its connectional affiliations differ from those of the ventral division (Winer, 1992); thus, it may have a role in multisensory processing.

The topographic distribution of thalamic labeling supports the physiological observation with regard to frequency specific organization. The anterior auditory field (AAF) experiments labeled mainly the lateral, low-to-middle frequency regions in the ventral division (Figs. 4E, 5E), whereas the AI deposits labeled the more medial, high-frequency part of the ventral division (Aitkin and Webster, 1972). In Pol, the labeling in the lowest-

frequency experiments should extend most rostrally, which it does (Fig. 5H: 0.94%), whereas the higher-frequency deposit labeled more caudal Pol (Fig. 3H: 0.81%). It is less obvious how Pol relates to nonprimary areas, with whom its connections seem just as orderly (Figs. 7, 8), nor is it clear why there is no input from limbic-related regions of nonprimary cortex (Figs. 9, 10, 14), insofar as it is an entity independent of the ventral division. This nucleus, thus, seems to have an ambiguous position in any hierarchy of thalamocortical processing. On the one hand, its neurons have a clear organization of best frequency and monosynaptic midbrain and cortical connection appropriate to an auditory designation as primary or lemniscal. On the other hand, its extra-auditory projections and the presence of a second, independent representation of best frequency distinguish it from the principal part of the ventral division. Resolution of these issues will require further study.

Reciprocity of thalamic and cortical projections

Despite the prominence of connectional reciprocity, its role as an organizing principle in thalamic function is obscure. Each primary sensory thalamic nucleus has strong connectional reciprocity with the cerebral cortex. Substantial areas of auditory thalamocortical-corticothalamic reciprocity were seen in prior work in cat (Colwell, 1975) and rat (Winer and Larue, 1987). The present results confirm the earlier findings and extend them. Every experiment also revealed some nonreciprocal projections. Sometimes these were moderate in size and within ≈1 mm of significant reciprocal labeling (Fig. 6F: Ov) while in other sections, nonreciprocal foci of transport were remote from reciprocal projections and included both CT (Fig. 6G: Ov) and TC (Fig. 6D: M) labeling. This outcome was most apparent after injections in the nontonotopic fields, where nearly all cases had such zones. Perhaps the nontonotopic areas have more divergent projections. Autoradiographic and axonal degeneration studies of the visual corticogeniculate projection from cat areas 17, 18, and 19 found that input from area 17 was heavier and more evenly distributed (Updyke, 1975). This finding suggests areal differences in projection strength. Our data suggest that every cortical area and each thalamic nucleus participate in the corticothalamic system, albeit in different degrees. Although descending projections in nontopographic nuclei are more divergent (Bourassa et al., 1995), this cannot predict the outcome of the present study or the high overall degree of reciprocity. Injecting areas without cochleotopic organization (area AII, Fig. 7; but see Galazyuk, 1990) produced a labeling pattern just as discrete and focal as did deposits in tonotopic areas (area AAF, Fig. 4). This finding suggests that some unknown axis of organization, independent of tonotopic arrangement, controls this relation. A third possibility is that differences in corticothalamic axonal morphology could underlie the various projection patterns. The negative evidence bearing on this hypothesis is that, in BDA experiments, in which axon terminals alone were charted (see example in Fig. 5), their distribution was virtually identical to that of the corresponding WGA-HRP case (Fig. 4). Perhaps the branching patterns of corticofugal axons from primary and nonprimary areas are similar, despite areal and nuclear differences in terminal architecture.

There are certainly cortical and nuclear differences in the populations of CT axons: some of the largest terminals arose from AII projection cells and from other nonprimary regions and their boutons were found principally in the dorsal division (Bajo et al., 1995). Nonetheless, these terminal fields were as specific and focal as those ending in the ventral division (Winer et al., 1999). Evidence from autoradiographic studies indicates that the corticofugal input to the lateral posterior nucleus was not always larger than the matching terminal zone in the lateral geniculate body in the same experiment (Updyke, 1977), despite massive differences in the topography of visual field representation and the receptive field domains of single neurons in these two nuclei. This result is in accord with the present findings, and confirms that areas whose sensory representation may be less precise than that in primary cortex nonetheless have highly specific projections. This has interesting developmental implications, because the establishment of such connections must be independent of peripheral topography in a sensory epithelium.

Among the most striking examples of extra-auditory nonreciprocity is the hypothalamic projection to the insular cortex (Fig. 9D,G,H), an input without a matching corticohypothalamic connection. This suggests that the cortex, or at least insular cortex, cannot influence or veto hypothalamocortically mediated processes directly. For reasons that are not clear, another study of insular cortex connections did not describe this projection (Clascá et al., 1997). In any event, reciprocity remains an intriguing principle in search of an explanation and a function (Deschênes et al., 1998).

Cortical relations with the thalamic intralaminar system

We found a small but consistent projection from some cortical fields to the thalamic intralaminar nuclei. In three experiments (Figs. 8–10 and in others not shown) there was mixed labeling in the subparafascicular or suprapeduncular nuclei, transport that sometimes extended medially into the posterior intralaminar complex (Winer et al., 1988). Neurons here have long, sparsely branched dendrites that would be ideal for integrating input from many sources. The experiments with such labeling involved deposits in insular, temporal, or the posterior ectosylvian cortex, areas with multisensory affiliations (Loe and Benevento, 1969; Olson and Graybiel, 1987). This suggests that, among the nontonotopically organized fields (Fig. 14), AII alone has virtually no connections with these nuclei (present results, Fig. 15; see also Bentivoglio et al., 1983) other than an occasional projection neuron (Fig. 7G). Many posterior intralaminar nucleus neurons in the rat have axons that branch extensively, with divergent and robust input to the globus pallidus and striatum, and a weaker projection to the cortex (Deschênes et al., 1996). If analogous axonal divergence exists in the cat corticothalamic system, this might allow a comparatively small population of cortical neurons to exert widespread influence on premotor pathways. These effects could be complementary to those from the suprageniculate nucleus to the caudate nucleus (Hu and Jayarman, 1986). The ability of corticofugal neurons to synchronize oscillations in their thalamic target nuclei endows the corticothalamofugal pathway with functional importance (Steriade, 1997). These neurons may also have a local role by virtue of their

intracortical axonal collaterals (Ferster and Lindström, 1985).

Nonprimary cortical areas, thus, may participate in four different connectional systems: (1) an auditory-related function through their medial geniculate body projections; (2) an integrative role served by input to multisensory thalamic nuclei; (3) influences on premotor and perhaps cognitive processes by means of basal telencephalic projections; and (4) access to broad cortical territories by way of their relation with the thalamic intralaminar system that might affect vigilance in rodents (Herkenham, 1980). For each scenario, the functional impact of cortical input to the intralaminar nuclei could belie their comparatively small size.

Functional aspects of the corticogeniculate system

Prior studies revealed a wide range of thalamic outcomes from cooling or stimulating cortex (summarized in Winer, 1992). Electrical stimulation of AI evoked antidromic, transsynaptic, reverberatory, or inhibitory effects (Aitkin and Dunlop, 1969), whereas cooling checked the late reverberatory response but did not alter auditory thalamic discharge rate (Ryugo and Weinberger, 1976). In awake cats, cortical cooling affected the spontaneous rate of arousal-related changes, suggesting that the CT system has a behaviorally state-dependent role (Orman and Humphrey, 1981).

Reversibly inactivating AI caused profound changes in the excitability of medial geniculate body neurons in a study comparing the response patterns in the auditory thalamus and the thalamic reticular nucleus (Villa et al., 1991). Specific changes induced in the ventral division by cortical cooling include decreased firing rates in most neurons and an increased signal-to-noise ratio. Blockade revealed two types of unit response along every dimension tested, leading to the conclusion that the CT system had a variety of effects on its target population. In dorsal division nuclei and Pol, inactivation had similar effects on both evoked and spontaneous discharges. Although these authors found it surprising that AI stimulation elicited any change in the dorsal division, the present results (Fig. 14) confirm that an appropriate anatomical substrate for such an effect exists. The main conclusions were that all auditory thalamic neurons were affected, that AI has chiefly an excitatory CT effect, and that significant divisional differences occur. It has been proposed that thalamic neuronal assemblies are responsible for adaptive filtering (Villa and Abeles, 1990). Critical emphasis was placed on the cortico-reticulo-thalamic circuit (Villa et al., 1991). This idea is supported by the demonstration that perigeniculate-elicited IPSPs can activate both $GABA_A$- and $GABA_B$-mediated mechanisms (Sanchez-Vives and McCormick, 1997) that affect the excitability of lateral geniculate body principal neurons and could modulate levels of vigilance or responsiveness to afferent signals (Kim et al., 1997). Each of these findings suggest a dynamic role for the CT system in synchronizing thalamic output (Contreras and Steriade, 1996).

A second and less direct route exists for possible cortical modulation of the auditory thalamus. This pathway involves inferior colliculus subdivisions in which cortical projections are among the strongest influences and in which brainstem input is reduced relatively and concomitantly. Thus, the dorsal and caudal cortices of the inferior colliculus, and the lateral nucleus, are each a major recipient of cortical input (Winer et al., 1998). These midbrain nuclei project, in turn, upon several subdivisions of the medial geniculate body (Calford and Aitkin, 1983; Winer et al., 1996).

Comparing and contrasting corticothalamic and corticocollicular systems

Perhaps the sharpest contrast between the CT and the corticocollicular (CC) projections is the robust projection to the ventral division of the medial geniculate body and the far smaller CC input to the central nucleus of the inferior colliculus (Figs. 12–15; Andersen et al., 1980c). The ventral division receives a strong projection from the central nucleus (Calford and Aitkin, 1983). Transmission through the central nucleus is not influenced directly by descending input, except through possible polysynaptic association circuits in rats from the lateral nucleus to the central nucleus (Saldaña and Merchán, 1992) that would add one or more synaptic delays. On balance, the CC projections are more divergent than CT input. The CC system seems to target midbrain nuclei whose ascending projections end primarily in the dorsal division nuclei and the medial division (Fig. 12A–C: 3), which themselves project mainly to nonprimary cortex and to the subcortical forebrain (Winer, 1992; Winer et al., 1998).

It is more difficult to contrast the effects of stimulating or inactivating the cerebral cortex on the inferior colliculus or the medial geniculate body because the consequences are complex. Corticocollicular stimulation evoked postsynaptic potentials of either or both types (excitatory and inhibitory PSPs) or sequences of these (Mitani et al., 1983; Syka and Popelář, 1984). Cortically elicited responses in conjunction with GABAergic blockade raised collicular thresholds, reduced response areas, and improved the sharpness of collicular tuning (Sun et al., 1996). Although similar effects can be elicited in the thalamus, such stimulation necessarily includes the inferior colliculus and, therefore, may affect the medial geniculate body transsynaptically. The effect of cortical stimulation or inactivation on the receptive fields of midbrain or thalamic neurons is robust and can be long-lasting. Moreover, bat cortical neurons matched in frequency with their subcortical counterparts facilitated the latter's responses and inhibited those of unmatched neurons (Zhang et al., 1997). Such effects might help to account for the extraordinary precision of corticothalamic-thalamocortical reciprocity, and it suggests a role for nonreciprocal corticofugal projections in the mediation of off-frequency lateral inhibition. It remains to examine the effect of corticogeniculate input on thalamocortical excitability after inactivation of the inferior colliculus.

Diversity and unity of corticothalamic systems

The evidence of divergent connections and of several types of descending axon supports the idea of more than one auditory corticogeniculate pathway, without being able to specify at present the different types of information each channel might carry. Further corroborative evidence for parallel pathways is that the CT cells of origin are heterogeneous morphologically and have three sublaminar origins in AI, each of which is independent of, although sometimes overlapping with, the CC system (Winer and Prieto, unpublished observations; for an ex-
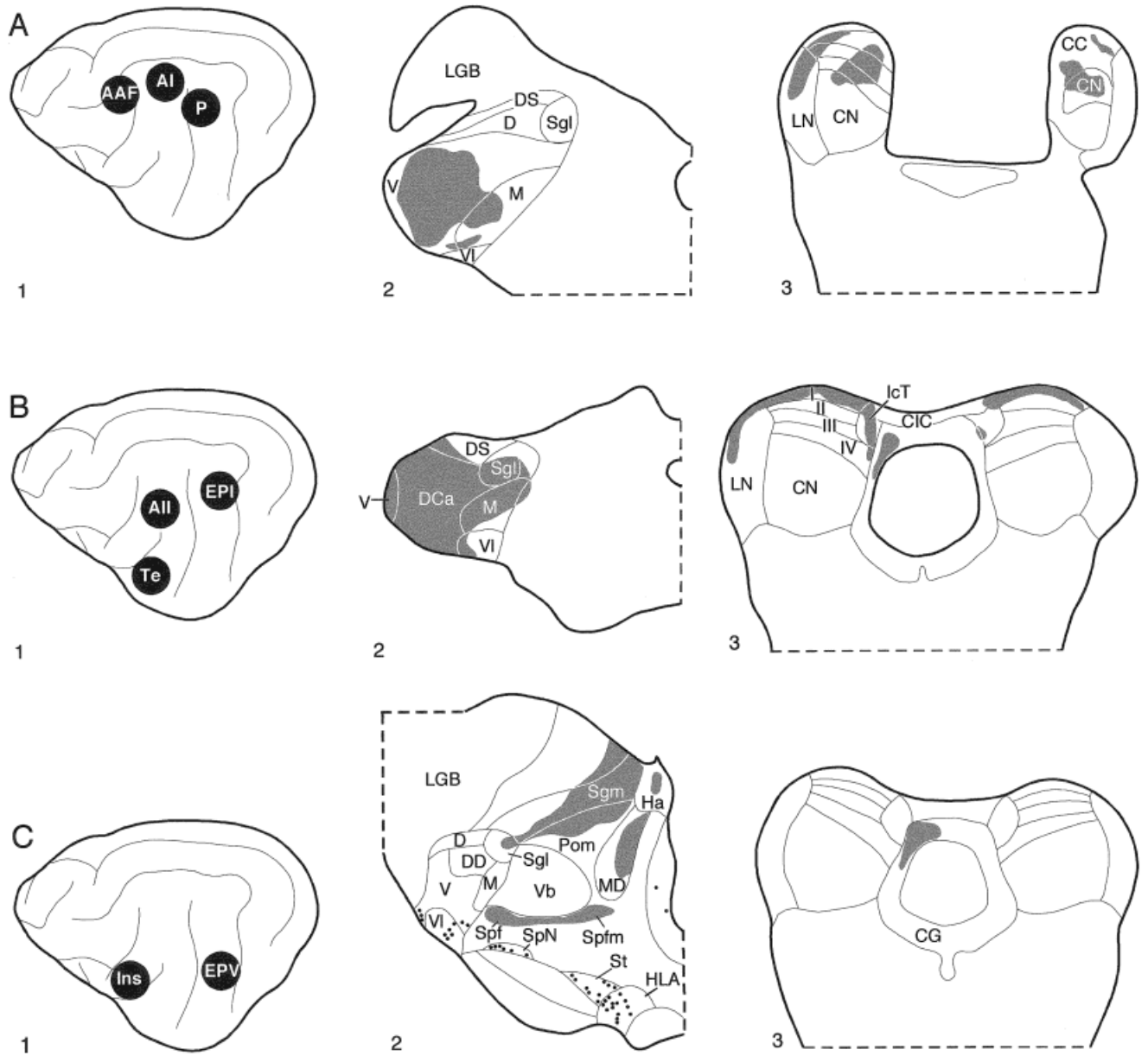
Fig. 12. Comparisons of anterograde terminal labeling patterns from various auditory cortical fields (1) in the auditory thalamus (2) and midbrain (3). **A:** The primary auditory cortex pattern involved strongly reciprocal projections between tonotopically organized cortical areas (1: AAF,AI, etc.) and their thalamic counterparts, mainly in the ventral division (2: V). The corticogeniculate projections were always heaviest and topographic, whereas the corticocollicular input was bilateral, nucleus-specific, and had no evident topographic relation with its target. **B:** The nonprimary pattern was embodied by the projections of areas AII and the caudodorsal parts of the posterior ectosylvian gyrus. The thalamic targets were principally the dorsal division and the associated caudal dorsal nucleus of the medial geniculate body and the lateral part of the suprageniculate nucleus. The corresponding corticocollicular labeling was, again, lighter, equally nucleus-specific, and it targeted mainly the superficial dorsal cortex (layer I) preferentially. **C:** The polysensory/paralimbic corticofugal pattern was distinct from the primary and nonprimary patterns. In the auditory thalamus, chiefly the rostral pole and the medial part of the suprageniculate nucleus (2: Sgm) and the rostral thalamic intralaminar system (2: Spf,Spfm,SpN) were labeled, as well as limbic-related thalamic territories (2: MD) and portions of the hypothalamus; the labeling in the latter was exclusively retrograde and was included here to emphasize global differences in projection patterns. In contrast to the primary and nonprimary projection systems, polysensory/paralimbic projections to the inferior colliculus were absent. See Figures 14,15 for further summaries.

ception in the rat, see also Deschênes et al., 1994). Further evidence is the diversity of CT axonal structure, which range from very fine fibers with delicate endings (Ojima, 1994; Ojima et al., 1996) to some of the largest terminals in the mammalian brain (Winer et al., 1999). If axonal terminal size is a reliable criterion for suggesting plausible functional distinctions, this suggests a far broader range of actions for the CT system than does the much
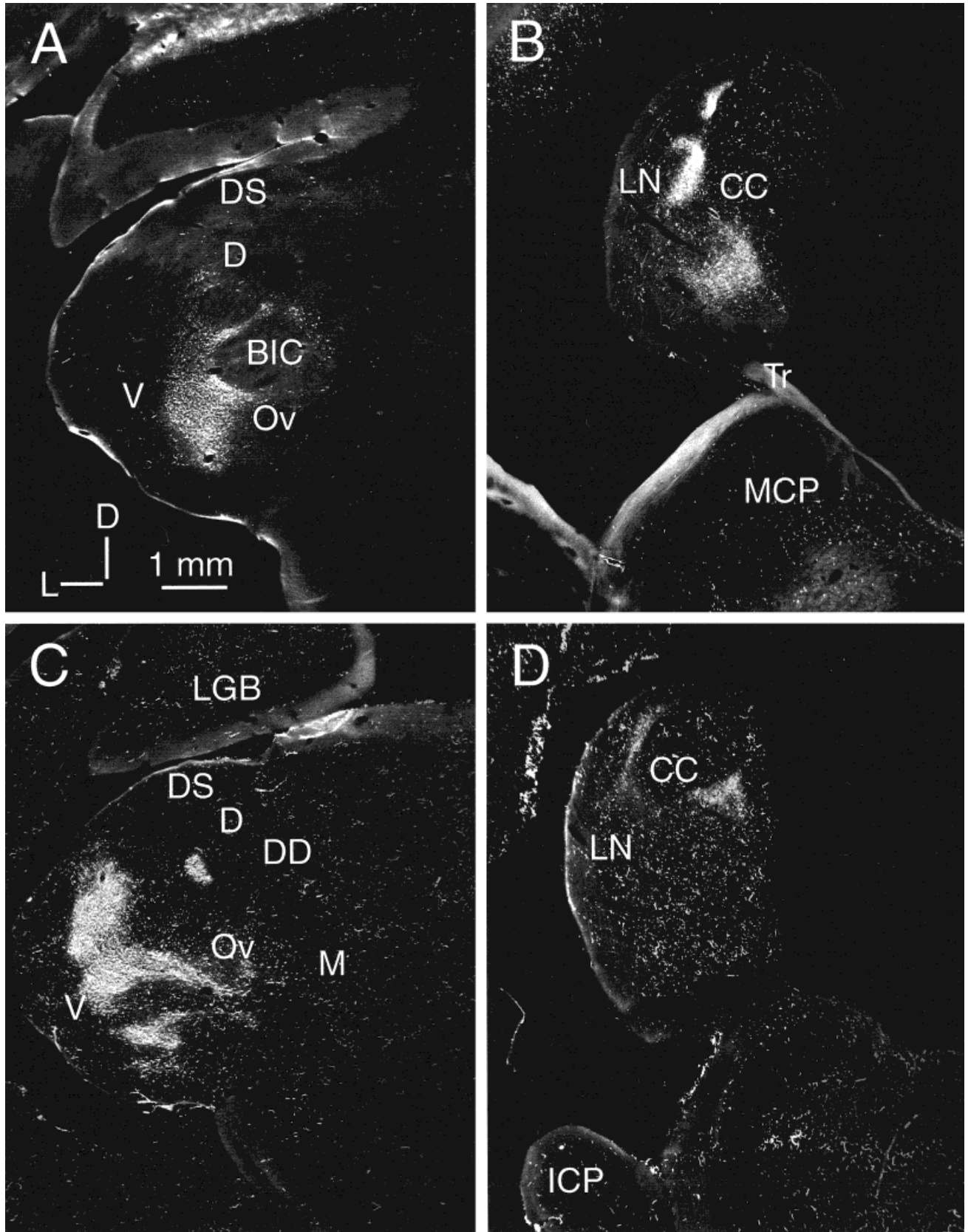
Fig. 13. Contrasting patterns of corticogeniculate-geniculocortical (A,C) and corticocollicular (B,D) projections from the same experiments. Protocol for A–D: See legend for Figure 11; ×16. **A:** Injections of wheat germ agglutinin conjugated to horseradish peroxidase (WGA-HRP) in AI (Fig. 3A) filled the central part of the ventral division (V,Ov) with mixed labeling, and demonstrated weaker projections to the dorsal (Fig. 3E: D) and medial (Fig. 3E: M) divisions. The labeling in each division was continuous. These images and those in Figure 11 were not retouched. **B:** The corticocollicular labeling was, in contrast, anterograde only, bilateral (not illustrated), patchy, and involved both the caudal collicular cortex (CC) and the lateral nucleus (LN), two nuclei differing in structure and connections (Aitkin, 1986). **C:** Deposits in the anterior auditory field (AAF; Fig. 3A) also labeled many ventral division cells and axons (Fig. 4D: V) and fewer in the medial division (Fig. 4D: M). **D:** The corticocollicular input was more focal and discrete than that in the prior experiment, with bursts of labeling >1 mm apart and centered in different collicular territories.

Other Studies of Auditory Corticothalamic Projections

CORTICAL AREA

		AI	AAF	P	VP	Ve	AII	EPI	EPD	EPP	Ins	Te	SF
		TONOTOPIC					NONTONOTOPIC						
M E D I A L G E N I C U L A T E B O D Y	V	1 2 4 5	1	1 4	1	1	1	1 4	1	1	1		
	Ov	1 2 4 5	1 4	1 4	1	1	1	1	1	1	1	1	
	Pol	1 2 4	1 4	1	1	1	1	1	1	1	1 2	1 2	
	DS	1	1 3	1 4			1 2 4 5	1 2	1	1	1 2 6	1 2 2	2
	D	1		1 4	1	1	1 2 4 5	1 2 5	1	1	1 2 6	1 2 2	2
	DD	4 5	5	4			1 2 4 5	1 2 5	1 3	1	1 2	1 2	1 5
	DCa						1 2 4 5	1 2	1	1	1 2	1 2 3	1
	Sgl						1	1	1	1	1 2 3	1 2	1
	Sgm		3				2	1	1 3	1	1 2 3 6	1 2	1
	Vl		1	1		1	1 2 4	1	1	1	1 6	1	1
	PL							1	1	1		1	
	M	1 2 4 5	1	1 4	1	1	1 2 5	1 2 5	1 3	1	1 2	1 2	1 5
O T H E R	Spf/SpN							1	1	1	1 2a 6a	1 2a	
	Pul							1	1 3	1			
	LP							1	1	1			
	LD												
	MD										1		
	HDA										1		
	Other										2a 6a	2a	

TARGET

Key
1 Present results.
2 Diamond et al. (1969).
3 Cranford et al. (1976).
4 Andersen et al. (1980a).
5 Pontes et al. (1975).
6 Clascá et al. (1997).

Notes
2a To the suprapeduncular nucleus
6a To the lateral medial, limitans, mediodorsal, and ventromedial nuclei

Fig. 14. Summary of other studies of cat auditory corticothalamic projections. There is considerable concordance between the present results and those obtained in silver degeneration studies (Diamond et al., 1969) or autoradiographic investigations (Pontes et al., 1975) or when autoradiography was combined with anterogradely transported horseradish peroxidase (Andersen et al., 1980a). The lack of agreement among the investigations often reflects an incomplete lesion or injections too small to reveal a complete projection, or a choice of survival that was not optimal to produce a consistent pattern of labeling, or that a particular thalamic division was not recognized as a separate entity. The main patterns in the present study confirm those of prior work and have been extended to include other areas, such as the ventrolateral nucleus (Vl) or the caudal dorsal nucleus (DCa), which are now considered as architectonic entities with distinct patterns of connections and whose physiological organization awaits study.

more homogeneous axonal population characteristic of the corticocollicular axons in rat (Saldaña et al., 1996) and cat (Winer, unpublished observations). The target-specific nature of the projections also supports the idea that the CT projection is not unitary either in form or function. The diversity of axonal form is also in accord with the idea of multiple sublaminar CT origins (Kelly and Wong, 1981;

Winer and Prieto, unpublished observations), even though it remains to relate a specific source to a particular termination.

Assuming that there is more than one CT subsystem, it would be vital to understand how their actions are coordinated. One mechanism that could effect this is the multilaminar distribution of thalamic afferents (Huang and

Summary of Auditory Corticofugal Projections

A

CORTICAL FIELD

TONOTOPIC | NONTONOTOPIC

TARGET — MEDIAL GENICULATE BODY / OTHER

	AI	AAF	P	VP	Ve	AII	EPP	EPD	EPI	Ins	Te	SF
V	heavy	heavy	heavy	heavy	heavy	light		light	light		light	light
Ov	heavy	heavy	heavy	medium	medium	light		medium	heavy		light	
Pol	light	heavy	medium	light	medium	medium	light	heavy	medium			
DS	light					medium	light	light	medium		heavy	medium
D	medium	light	medium	medium	light	heavy	heavy	heavy	heavy	light	heavy	heavy
DD			light			heavy	heavy	heavy	heavy	heavy	heavy	heavy
DCa						heavy		heavy	medium	heavy	heavy	
Sgl						medium	medium	heavy	heavy	heavy	medium	heavy
Sgm							heavy	heavy	heavy	heavy	light	
Vl		light	medium	light		medium		medium	medium	light	heavy	
PL							light	light	light	light		
M	light	medium	light	light	light	medium	light	medium	heavy	heavy	heavy	heavy
Spf/SpN								medium	light	light	light	medium
Pul							medium	heavy	light			
LP							heavy	medium	medium			
LD							medium	light				
Other						light[3]				medium[1]		medium[2]

Key
- ● heavy
- ● medium
- · light

B

INFERIOR COLLICULUS / OTHER

	AI	AAF	P	VP	Ve	AII	EPP	EPD	EPI	Ins	Te	SF
CN	light	light		light	light		medium	medium				
DC I	light	light	light	light	light	medium		medium	light	light	medium	
DC II	medium	heavy	heavy	medium	medium	light		light	light		medium	
DC III	heavy	heavy	medium	medium	medium	light		light	light		medium	
DC IV	medium	medium	light	light	medium			light	light	light	medium	
CC	heavy	medium	medium	medium	heavy	medium		light	light		heavy	light
LN	medium	medium	medium	light	medium	medium		light	light		light	medium
IcT		light		light		medium		light	light		heavy	medium
RP				medium								medium
SC						light	light	heavy	heavy	light		medium
Sa	light	light	light	light		light		heavy	medium	heavy	light	light
CG								light	light	heavy	light	
Cu										heavy		

Notes
1 Medial dorsal nucleus
2 Lateral mesencephalic nucleus
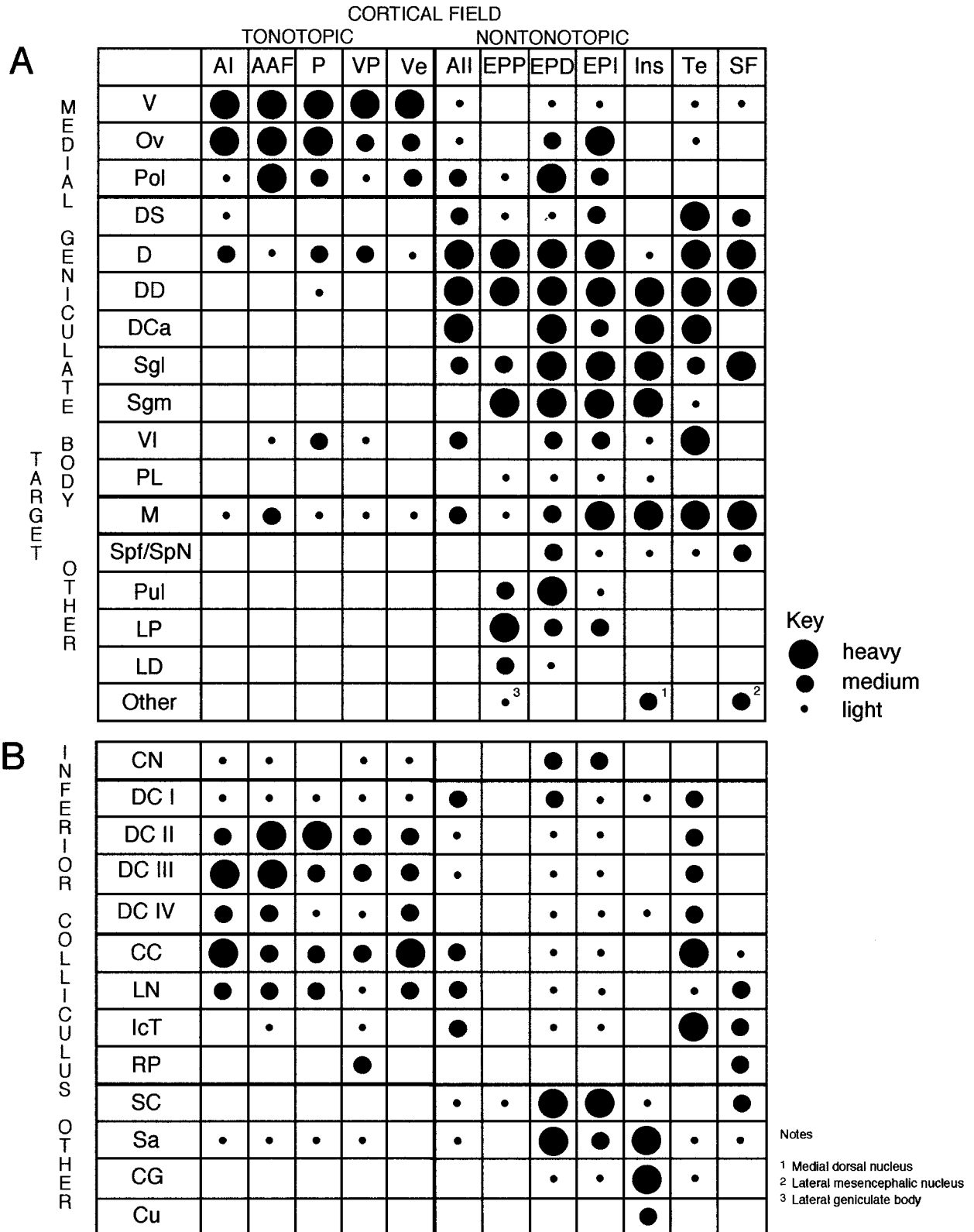3 Lateral geniculate body

Fig. 15. Summary of auditory corticofugal projections to the medial geniculate body (A) and inferior colliculus (B). **A:** Qualitative estimates of the strength of anterograde labeling after tracer deposits confined to one cortical area. The values were derived by examining all of the intermediate plots of labeling (from which the sections illustrated were chosen) and seriating projection density within and across nuclei. This included the biotinylated dextran amines experiments (Fig. 5; see also Winer et al., 1999), with which the wheat germ agglutinin conjugated to horseradish peroxidase results were in close agreement (Fig. 4). Values at or near a boundary were assigned the lower value. Three patterns of projection were recognized. The first involved all the TONOTOPIC areas and their connections with the ventral division, the rostral pole/lateral segment of the posterior nucleus, and limited parts of the dorsal division; these connections were strong, topographic, and labeled comparatively few targets. The second, NONTONOTOPIC pattern involved the dorsal division principally; these projections were far more divergent than those from TONOTOPIC areas. The third arrangement was division-specific: almost all cortical areas projected to the medial division, although this input was much weaker and more variable than that of the first two projection systems. **B:** In contrast to the CT projection, the corticocollicular (CC) system projects outside the lemniscal hub of the midbrain (central nucleus; CN), it was more variable in terminal density, and there was a far smaller contribution from NONTONOTOPIC areas. For further analysis, see the Discussion section.

Winer, 2000), which may have synaptic access to the very CT neurons that project reciprocally to them in mice (White and Hersch, 1982), monkeys (Hashikawa et al., 1995), and other species (Jones, 1985). A second substrate for translaminar activation is the local axonal branches of CT neurons in layers V and VI (Ferster and Lindström, 1985). Such intrinsic projections, in conjunction with thalamic afferents, could coordinate the discharge patterns in this and other corticofugal systems to achieve temporal unity of action.

ACKNOWLEDGMENTS

LITERATURE CITED

Adams JC. 1981. Heavy metal intensification of DAB-based HRP reaction product. J Histochem Cytochem 29:775.

Aitkin LM. 1973. Medial geniculate body of the cat: responses to tonal stimuli of neurons in medial division. J Neurophysiol 36:275–283.

Aitkin LM. 1986. The auditory midbrain: structure and function in the central auditory pathway. Clifton, NJ: Humana Press.

Aitkin LM, Dunlop CW. 1968. Interplay of excitation and inhibition in the cat medial geniculate body. J Neurophysiol 31:44–61.

Aitkin LM, Dunlop CW. 1969. Inhibition in the medial geniculate body of the cat. Exp Brain Res 7:68–83.

Aitkin LM, Prain SM. 1974. Medial geniculate body: unit responses in the awake cat. J Neurophysiol 37:512–521.

Aitkin LM, Webster WR. 1972. Medial geniculate body of the cat: organization and responses to tonal stimuli of neurons in ventral division. J Neurophysiol 35:365–380.

Andersen RA, Knight PL, Merzenich MM. 1980a. The thalamocortical and corticothalamic connections of AI, AII, and the anterior auditory field (AAF) in the cat: evidence for two largely segregated systems of connections. J Comp Neurol 194:663–701.

Andersen RA, Roth GL, Aitkin LM, Merzenich MM. 1980b. The efferent projections of the central nucleus of the inferior colliculus in the cat. J Comp Neurol 194:649–662.

Andersen RA, Snyder RL, Merzenich MM. 1980c. The topographic organization of corticocollicular projections from physiologically identified loci in AI, AII, and anterior auditory cortical fields of the cat. J Comp Neurol 191:479–494.

Bajo VM, Rouiller EM, Welker E, Clarke S, Villa AEP, de Ribaupierre Y, de Ribaupierre F. 1995. Morphology and spatial distribution of corticothalamic terminals originating from the cat auditory cortex. Hear Res 83:161–174.

Barone P, Clarey JC, Irons WA, Imig TJ. 1996. Cortical synthesis of azimuth-sensitive single-unit responses with nonmonotonic level tuning: a thalamocortical comparison in the cat. J Neurophysiol 75:1206–1222.

Benedek G, Fischer-Szátmári L, Kovács G, Perényi J, Katoh YY. 1996. Visual, somatosensory and auditory modality properties along the feline suprageniculate-anterior ectosylvian sulcus/insular pathway. Prog Brain Res 90:325–334.

Benedek G, Perény J, Kovács G, Fischer-Szátmári L, Katoh YY. 1997. Visual, somatosensory, auditory and nociceptive modality properties in the feline suprageniculate nucleus. Neuroscience 78:179–189.

Beneyto M, Winer JA, Larue DT, Prieto JJ. 1998. Auditory connections and neurochemical organization of the sagulum. J Comp Neurol 401:329–351.

Bentivoglio M, Molinari M, Minciacchi D, Macchi G. 1983. Organization of the cortical projections of the posterior complex and intralaminar nuclei of the thalamus as studied by means of retrograde tracers. In: Macchi G, Rustioni A, Spreafico R, editors. Somatosensory integration in the thalamus. Amsterdam: Elsevier Publishing Company. p 337–363.

Berman AL, Jones EG. 1982. The thalamus and basal telencephalon of the cat: a cytoarchitectonic atlas with stereotaxic coordinates. Madison, WI: University of Wisconsin Press.

Bourassa J, Pinault D, Deschênes M. 1995. Corticothalamic projections from the cortical barrel field to the somatosensory thalamus in rats: a single-fibre study using biocytin as an anterograde tracer. Eur J Neurosci 7:19–30.

Bowman EM, Olson CR. 1988a. Visual and auditory association areas of the cat's posterior ectosylvian gyrus: cortical afferents. J Comp Neurol 272:30–42.

Bowman EM, Olson CR. 1988b. Visual and auditory association areas of the cat's posterior ectosylvian gyrus: thalamic afferents. J Comp Neurol 272:15–29.

Calford MB, Aitkin LM. 1983. Ascending projections to the medial geniculate body of the cat: evidence for multiple, parallel auditory pathways through the thalamus. J Neurosci 3:2365–2380.

Casseday JH, Kobler JB, Isbey SF, Covey E. 1989. Central acoustic tract in an echolocating bat: an extralemniscal auditory pathway to the thalamus. J Comp Neurol 287:247–259.

Clarey JC, Barone P, Imig TJ. 1992. Physiology of thalamus and cortex. In: Popper AN, Fay RR, editors. Springer handbook of auditory research, Vol. 2, the mammalian auditory pathway: neurophysiology. New York: Springer-Verlag. p 232–334.

Clascá F, Llamas A, Reinoso-Suárez F. 1997. Insular cortex and neighboring fields in the cat: a redefinition based on cortical microarchitecture and connections with the thalamus. J Comp Neurol 384:456–482.

Colwell S. 1975. Thalamocortical-corticothalamic reciprocity: a combined anterograde-retrograde tracer technique. Brain Res 92:443–449.

Contreras D, Steriade M. 1996. Spindle oscillation in cats: the role of corticothalamic feedback in a thalamically generated rhythm. J Physiol (Lond) 490:159–179.

Crabtree JW. 1998. Organization in the auditory sector of the cat's thalamic reticular nucleus. J Comp Neurol 390:167–182.

Cudeiro J, Sillito AM. 1996. Spatial frequency tuning of orientation-discontinuity-sensitive corticofugal feedback to the cat lateral geniculate nucleus. J Physiol (Lond) 490:481–492.

Deschênes M, Bourassa J, Pinault D. 1994. Corticothalamic projections from layer V cells in rat are collaterals of long-range corticofugal axons. Brain Res 664:215–219.

Deschênes M, Bourassa J, Doan VD, Parent A. 1996. A single-cell study of the axonal projections arising from the posterior intralaminar thalamic nuclei in the rat. Eur J Neurosci 8:329–343.

Deschênes M, Veinante P, Zhang Z-W. 1998. The organization of corticothalamic projections: reciprocity versus parity. Brain Res Brain Res Rev 28:286–308.

Diamond IT, Jones EG, Powell TPS. 1969. The projection of the auditory cortex upon the diencephalon and brain stem of the cat. Brain Res 15:305–340.

Diehl JJ, Winer JA. 1996. Contrasting auditory corticofugal projections to the inferior colliculus and medial geniculate body. Proc Soc Neurosci 22:1069.

Ferster D, Lindström S. 1985. Synaptic excitation of neurones in area 17 of the cat by intracortical axon collaterals of cortico-geniculate cells. J Physiol (Lond) 367:233–252.

Fitzpatrick D, Usrey WM, Schofield BR, Einstein G. 1994. The sublaminar organization of corticogeniculate neurons in layer 6 of macaque striate cortex. Vis Neurosci 11:307–315.

Fitzpatrick DC, Batra R, Stanford TR, Kuwada S. 1997. A neuronal population code for sound localization. Nature 388:871–874.

Frigyesi T, Rinvik E, Yahr MD, editors. 1972. Corticothalamic projections and sensorimotor activities. New York: Raven Press.

Funke K, Nelle E, Li B, Wörgötter F. 1996. Corticofugal feedback improves the timing of retino-geniculate signal transmission. Neuroreport 7:2130–2134.

Galazyuk AV. 1990. Tonotopic organization of the ventrorostral zone of the auditory region AII in cats. Neurophysiology 22:139–144.

Hashikawa T, Molinari M, Rausell E, Jones EG. 1995. Patchy and laminar terminations of medial geniculate axons in monkey auditory cortex. J Comp Neurol 362:195–208.

Herkenham M. 1980. Laminar organization of thalamic projections to rat neocortex. Science 207:532–534.

Hu H, Jayarman A. 1986. The projection pattern of the suprageniculate nucleus to the caudate nucleus in cats. Brain Res 368:201–203.

Huang CL. 1999. Cortical projections and GABAergic organization of the cat medial geniculate body. Doctoral thesis, Univ Calif at Berkeley.

Huang CL, Winer JA. 2000. Auditory thalamocortical projections in the cat: laminar and areal patterns of input. J Comp Neurol 427:302–331.

Huang CL, Larue DT, Winer JA. 1999. GABAergic organization of the cat medial geniculate body. J Comp Neurol 415:368–392.

Imig TJ, Morel A. 1984. Topographic and cytoarchitectonic organization of thalamic neurons related to their targets in low-, middle-, and high-frequency representations in cat auditory cortex. J Comp Neurol 227: 511–539.

Imig TJ, Morel A. 1985. Tonotopic organization in lateral part of posterior group of thalamic nuclei in the cat. J Neurophysiol 53:836–851.

Jones EG. 1985. The thalamus. New York: Plenum Press.

Jones EG, Powell TPS. 1973. Anatomical organization of the somatosensory cortex. In: Iggo A, editor. Handbook of sensory physiology, Vol. II, somatosensory system. Berlin: Springer-Verlag. p 579–620.

Kawamura K. 1971. Variations of the cerebral sulci of the cat. Acta Anat 80:204–221.

Kelly JP, Wong D. 1981. Laminar connections of the cat's auditory cortex. Brain Res 212:1–15.

Kim U, Sanchez-Vives MV, McCormick DA. 1997. Functional dynamics of GABAergic inhibition in the thalamus. Science 278:130–134.

Knight PL. 1977. Representation of the cochlea within the anterior auditory field (AAF) of the cat. Brain Res 130:447–467.

Krieg WJS. 1963. Connections of the cerebral cortex. Evanston, IL: Brain Books.

Loe PR, Benevento LA. 1969. Auditory-visual interaction in single units in the orbito-insular cortex of the cat. Electroenchphalogr Clin Neurophysiol 26:395–398.

McClurkin JW, Optican LM, Richmond BJ. 1994. Cortical feedback increases visual information transmitted by monkey parvocellular lateral geniculate nucleus neurons. Vis Neurosci 11:601–617.

Meredith MA, Clemo HR. 1989. Auditory cortical projection from the anterior ectosylvian sulcus (field AES) to the superior colliculus in the cat: an anatomical and electrophysiological study. J Comp Neurol 289:687–707.

Mesulam M-M. 1978. Tetramethyl benzidine for horseradish peroxidase neurohistochemistry: a non-carcinogenic blue reaction-product with superior sensitivity for visualizing neural afferents and efferents. J Histochem Cytochem 26:106–117.

Mesulam M-M, Pandya DN. 1973. The projections of the medial geniculate complex within the Sylvian fissure of the rhesus monkey. Brain Res 60:315–333.

Mitani A, Shimokouchi M, Nomura S. 1983. Effects of stimulation of the primary auditory cortex upon colliculogeniculate neurons in the inferior colliculus of the cat. Neurosci Lett 42:185–189.

Morest DK. 1964. The neuronal architecture of the medial geniculate body of the cat. J Anat (Lond) 98:611–630.

Morest DK. 1965. The laminar structure of the medial geniculate body of the cat. J Anat (Lond) 99:143–160.

Morest DK. 1971. Dendrodendritic synapses of cells that have axons: the fine structure of the Golgi type II cell in the medial geniculate body of the cat. Z Anat Entwicklungsgesich 133:216–246.

Niimi K, Matsuoka H. 1979. Thalamocortical organization of the auditory system in the cat studied by retrograde axonal transport of horseradish peroxidase. Adv Anat Embryol Cell Biol 57:1–56.

Ojima H. 1994. Terminal morphology and distribution of corticothalamic fibers originating from layers 5 and 6 of cat primary auditory cortex. Cereb Cortex 6:646–663.

Ojima H, Murakami K, Kishi K. 1996. Dual termination modes of corticothalamic fibers originating from pyramids of layers 5 and 6 in cat visual cortical area 17. Neurosci Lett 208:57–60.

Olson CR, Graybiel AM. 1987. Ectosylvian visual area of the cat: location, retinotopic organization, and connections. J Comp Neurol 261:277–294.

Orman SS, Humphrey GL. 1981. Effects of changes in cortical arousal and of auditory cortex cooling on neuronal activity in the medial geniculate body. Exp Brain Res 42:475–482.

Pandya DN, Rosene DL, Doolittle AM. 1994. Corticothalamic connections of auditory-related areas of the temporal lobe in the rhesus monkey. J Comp Neurol 345:447–471.

Pontes C, Reis FF, Sousa-Pinto A. 1975. The auditory cortical projections onto the medial geniculate body in the cat: an experimental anatomical study with silver and autoradiographic methods. Brain Res 91:43–63.

Prieto JJ, Winer JA. 1999. Neurons of layer VI in cat primary auditory cortex (AI): Golgi study and sublaminar origins of projection neurons. J Comp Neurol 404:332–358.

Przybyszewski AW. 1998. Does top-down processing help us to see? Curr Biol 8:R135–R139.

Reale RA, Imig TJ. 1980. Tonotopic organization in auditory cortex of the cat. J Comp Neurol 182:265–291.

Rose JE, Woolsey CN. 1949. The relations of thalamic connections, cellular structure, and evocable electrical activity in the auditory region of the cat. J Comp Neurol 91:441–466.

Rouiller EM, Rodrigues-Dagaeff C, Simm G, de Ribaupierre Y, Villa AEP, de Ribaupierre F. 1989. Functional organization of the medial division of the medial geniculate body of the cat: tonotopic organization, spatial distribution of response properties and cortical connections. Hear Res 39:127–146.

Rouiller EM, Capt M, Hornung JP, Streit P. 1990. Correlation between regional changes in the distributions of GABA-containing neurons and unit response properties in the medial geniculate body of the cat. Hear Res 49:249–258.

Ryugo DK, Weinberger NM. 1976. Corticofugal modulation of the medial geniculate body. Exp Neurol 51:377–391.

Saint Marie RL, Stanforth DA, Jubelier EM. 1997. Substrate for rapid feedforward inhibition of the auditory forebrain. Brain Res 765:173–176.

Saldaña E, Merchán MA. 1992. Intrinsic and commissural connections of the rat inferior colliculus. J Comp Neurol 319:417–437.

Saldaña E, Feliciano M, Mugnaini E. 1996. Distribution of descending projections from primary auditory neocortex to inferior colliculus mimics the topography of intracollicular projections. J Comp Neurol 371: 15–40.

Sanchez-Vives MV, McCormick DA. 1997. Functional properties of perigeniculate inhibition of dorsal lateral geniculate nucleus thalamocortical neurons in vitro. J Neurosci 17:8880–8893.

Schreiner CE, Cynader MS. 1984. Basic functional organization of second auditory cortical field (AII) of the cat. J Neurophysiol 51:1284–1305.

Society for Neuroscience 1991. Handbook for the use of animals in neuroscience research. Washington, DC: Society for Neuroscience.

Sousa-Pinto A. 1973. Cortical projections of the medial geniculate body in the cat. Adv Anat Embryol Cell Biol 48:1–42.

Steriade M. 1997. Synchronized activities of coupled oscillators in the cerebral cortex at different levels of vigilance. Cereb Cortex 7:583–604.

Stone J. 1983. Parallel processing in the visual system: the classification of retinal ganglion cells and its impact on the neurobiology of vision. New York, London: Plenum Press.

Sun X, Chen QC, Jen PH-S. 1996. Corticofugal control of central auditory sensitivity in the big brown bat, *Eptesicus fuscus*. Neurosci Lett 212: 131–134.

Syka J, Popelář, J. 1984. Inferior colliculus in the rat: neuronal responses to stimulation of the auditory cortex. Neurosci Lett 51:235–240.

Tusa RJ, Palmer LA, Rosenquist AC. 1981. Multiple cortical visual areas: visual field topography in the cat. In: Woolsey CN, editor. Cortical sensory organization, vol. 2: multiple visual areas. Clifton, NJ: Humana Press. p 1–31.

Updyke BV. 1975. The projections of cortical areas 17, 18, and 19 onto the laminae of the dorsal lateral geniculate nucleus of the cat. J Comp Neurol 163:377–396.

Updyke BV. 1977. Topographic organization of the projections from cortical areas 17, 18, and 19 onto the thalamus, pretectum and superior colliculus in the cat. J Comp Neurol 173:81–122.

Villa AEP, Abeles M. 1990. Evidence for spatio-temporal firing patterns within the auditory thalamus of the cat. Brain Res 509:325–327.

Villa AEP, Rouiller EM, Simm GM, Zurita P, de Ribaupierre Y, de Ribaupierre F. 1991. Corticofugal modulation of the information processing in the auditory thalamus of the cat. Exp Brain Res 86:506–517.

White EL, Hersch SM. 1982. A quantitative study of thalamocortical and other synapses involving the apical dendrites of corticothalamic projection cells in mouse SmI cortex. J Neurocytol 11:137–158.

Winer JA. 1984. Identification and structure of neurons in the medial geniculate body projecting to primary auditory cortex (AI) in the cat. Neuroscience 13:395–413.

Winer JA. 1992. The functional architecture of the medial geniculate body and the primary auditory cortex. In: Webster DB, Popper AN, Fay RR, editors. Springer handbook of auditory research, Vol. 1: the mammalian auditory pathway: neuroanatomy. New York, NY: Springer-Verlag. p 222–409.

Winer JA, Larue DT. 1987. Patterns of reciprocity in auditory thalamocortical and corticothalamic connections: study with horseradish peroxi-

dase and autoradiographic methods in the rat medial geniculate body. J Comp Neurol 257:282–315.

Winer JA, Morest DK. 1983a. The medial division of the medial geniculate body of the cat: implications for thalamic organization. J Neurosci 3:2629–2651.

Winer JA, Morest DK. 1983b. The neuronal architecture of the dorsal division of the medial geniculate body of the cat: a study with the rapid Golgi method. J Comp Neurol 221:1–30.

Winer JA, Morest DK. 1984. Axons of the dorsal division of the medial geniculate body of the cat: a study with the rapid Golgi method. J Comp Neurol 224:344–370.

Winer JA, Diamond IT, Raczkowski D. 1977. Subdivisions of the auditory cortex of the cat: the retrograde transport of horseradish peroxidase to the medial geniculate body and posterior thalamic nuclei. J Comp Neurol 176:387–418.

Winer JA, Morest DK, Diamond IT. 1988. A cytoarchitectonic atlas of the medial geniculate body of the opossum, *Didelphys virginiana*, with a comment on the posterior intralaminar nuclei of the thalamus. J Comp Neurol 274:422–448.

Winer JA, Saint Marie RL, Larue DT, Oliver DL. 1996. GABAergic feed-forward projections from the inferior colliculus to the medial geniculate body. Proc Natl Acad Sci USA 93:8005–8010.

Winer JA, Larue DT, Diehl JJ, Hefti BJ. 1998. Auditory cortical projections to the cat inferior colliculus. J Comp Neurol 400:147–174.

Winer JA, Larue DT, Huang CL. 1999. Two systems of giant axon terminals in the cat medial geniculate body: convergence of cortical and GABAergic inputs. J Comp Neurol 413:181–197.

Wörgötter F, Nelle E, Li B, Funke K. 1998. The influence of corticofugal feedback on the temporal structure of visual responses of cat thalamic relay cells. J Physiol (Lond) 509:797–815.

Yan J, Suga N. 1996a. Corticofugal modulation of time-domain processing of biosonar information in bats. Science 273:1100–1103.

Yan J, Suga N. 1996b. The midbrain creates and the thalamus sharpens echo-delay tuning for the cortical representation of target-distance information in the mustached bat. Hear Res 93:102–110.

Zhang Y, Suga N, Yan J. 1997. Corticofugal modulation of frequency processing in bat auditory system. Nature 387:900–903.